Journal of Hydrology: Regional Studies 44 (2022) 101229

Contents lists available at ScienceDirect

Journal of Hydrology: Regional Studies

journal homepage: www.elsevier.com/locate/ejrh

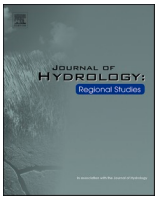

Meteorological and hydrological drought hazard, frequency and propagation analysis: A case study in southeast Australia

Gokhan Yildirim [a], Ataur Rahman [a,*], Vijay P. Singh [b,c,d]

[a] School of Engineering, Design and Built Environment, Penrith Campus, Western Sydney University, Sydney 2747, Australia
[b] Department of Biological and Agricultural Engineering, Texas A & M University, College Station, TX 77843-2117, USA
[c] Zachry Department of Civil & Environmental Engineering, Texas A & M University, College Station, TX 77843-2117, USA
[d] National Water and Energy Center, UAE University, Al Ain, United Arab Emirates

ARTICLE INFO

Keywords:
Standardized Precipitation Index (SPI)
Effective Drought Index (EDI)
Standardized Streamflow Index (SSFI)
Drought hazard
Drought frequency
Drought propagation

ABSTRACT

Study region: Southeast Australia.
Study focus: We investigated meteorological and hydrological drought characteristics using Standardized Precipitation Index (SPI), Standardized Streamflow Index (SSFI) and Effective Drought Index (EDI). Drought Hazard Index (DHI) was derived based on the probability of drought occurrence and Thiessen polygons using SPI/EDI, whereas Drought Frequency Index (DFI) was derived based on number of drought events, and data length using SPI, EDI, and SSFI. The modified Mann-Kendall test was applied to detect trends in streamflow data and hydrological droughts. Furthermore, correlation between meteorological and hydrological drought indices for different timesteps was assessed through Pearson's and Spearman's rank correlation analysis. Finally, the drought propagation time (DPT) from meteorological to hydrological drought was estimated by 'theory of run.'
New hydrological insights for the region: Our major findings include: (i) The spatial coverage of DHI and DFI, based on SPI/EDI, illustrate that mainly south and coastal regions of the study area are the most 'drought-prone' (ii) A considerable proportion of streamflow stations shows a significant trend of decrease in annual streamflow, with the most dominant year of abrupt change is 1996; (iii) Hydrological droughts are increasing in the study area; (iv) Performance of EDI with SSFI is found to be better than SPI at 3-month timestep; and (v) DPT can be found using 'theory of run' however, defined DPT cannot be directly applied to other regions.

1. Introduction

Global warming and increasing anthropogenic activities are generating extreme climate events around the world (Diffenbaugh et al., 2017; Trenberth, 2018; AghaKouchak et al., 2020). Drought is one of the most devastating (Mishra and Singh, 2010) and costly natural disasters (Bryant, 1991), which is still not fully understood (Van Lanen et al., 2013; Blauhut et al., 2015) and its causes and effects have not yet been adequately evaluated (Spinoni et al., 2014). There is no universally accepted definition of drought; however, it can be described as the deficiency of water relative to the statistical multi-year mean over a large area and for a large time span (e.g. a season, a year, or several years) (Palmer, 1965; Schneider, 1996). Review of various drought definitions can be found in Mishra and

* Corresponding author.
E-mail address: a.rahman@westernsydney.edu.au (A. Rahman).

https://doi.org/10.1016/j.ejrh.2022.101229
Received 6 May 2022; Received in revised form 26 August 2022; Accepted 3 October 2022
Available online 12 October 2022

Singh (2010). The water deficit propagates through the hydrological cycle and causes different types of droughts, which can be classified into four major categories, i.e., meteorological, hydrological, agricultural, and socio-economic (Palmer, 1965; Wilhite and Glantz, 1985). Among these, the first two drought types are of focus of this study. Hydrological drought, on the other hand, refers to streamflow deficiency in this study, since it is useful to address groundwater drought as a type of drought, which is not generally included in the classification of droughts (Mishra and Singh, 2010).

Australia, having a high rainfall variability, had experienced three major droughts in the recent past, the Federation drought (1895–1902), the World War II drought (1937–1945) and the Millennium drought (1997–2010). Due to its markedly seasonal and highly variable rainfall patterns, Australia is highly susceptible to droughts. More recently, southeast Australia experienced the driest two-year period between 2018 and 2019 on record (Hughes et al., 2020; Van Oldenborgh et al., 2021), and this extraordinary drought was the leading driver of the wildfires, the so called "Black Summer," in southeast Australia (Kemter et al., 2021).

Previous studies note that there has been a decreasing trend in rainfall and streamflow mainly in southern and south-eastern Australia (Murphy and Timbal, 2008; Timbal and Fawcett, 2013; Zhang et al., 2016; Hajani and Rahman, 2018; Vervoort et al., 2021). For instance, April to October rainfall covering the period of 2000–2019 has been found to decrease by 12% when compared to the 1900–1999 values (CSIRO and BOM, 2020), and the storage volumes in south-eastern Australia in this period were found to be the lowest in more than ten years (Bureau of Meteorology, 2020b). The deficiency of rainfall has long-term effects on both surface and groundwater resources.

The study area, covering NSW and VIC, comprises more than 60% of water supply over Australia and more than 90% of this water is sourced from surface water (Australian Bureau of Statistics, 2021). Therefore, investigation of hydrological drought and its link with meteorological drought have a vital importance in water security planning in the study area. Many researchers analyzed droughts in Australia, both at regional and national scales (White and O'Meagher, 1995; Mpelasoka et al., 2008; Ummenhofer et al., 2009; Rahmat et al., 2012; Gallant et al., 2013; Nazahiyah et al., 2014; Tian et al., 2019). Furthermore, many studies focused on what causes droughts in Australia (Verdon-Kidd and Kiem, 2009; CSIRO, 2010; Forootan et al., 2019; Wang et al., 2021). It has been found that four key climate drivers, Southern Annular Mode (SAM), El Nino/Southern Oscillation (ENSO), Indian Ocean Dipole (IOD), and Interdecadal Pacific Oscillation (IPO) cause a highly variable climate from year to year influencing the onset of drought in southeast Australia.

The intensity of a drought covering its frequency, areal extent, severity, and duration is essential for regional drought analysis (Mishra and Singh, 2009). For this purpose, drought indices are the best tool to monitor drought and to quantify its characteristics to provide information to decision-makers and to initiate a drought action plan. Hence, in this study we adopted Standardized Precipitation Index (SPI) (McKee et al., 1993) and Effective Drought Index (EDI) (Byun and Wilhite, 1999) for the identification of meteorological drought characteristics. SPI, a moving average based index, was recommended by World Meteorological Organization (2012). Both drought indices, SPI and EDI, have been widely applied around the world for drought monitoring (Hayes et al., 1999; Mishra and Desai, 2005; Sönmez et al., 2005; Cancelliere et al., 2007; Mishra and Singh, 2009; Deo et al., 2017; Caloiero, 2018; Rashid and Beecham, 2019; Li et al., 2021; Lohpaisankrit and Techamahasaranont, 2021; Malik et al., 2021; Salimi et al., 2021; Yildirim et al., 2022). Monthly rainfall is the only parameter for both indices. SPI can be computed at different timesteps, whereas EDI is a time independent index. Although the EDI was developed at a daily time step (Byun and Wilhite, 1999; Kim et al., 2009), it is an effective method to compute drought from monthly rainfall time series data (Smakhtin and Hughes, 2007; Akhtari et al., 2009; Dogan et al., 2012). In this study, Standardized Streamflow Index (SSFI) (Modarres, 2007; Telesca et al., 2012) was applied to compute hydrological drought. SSFI has a calculation process similar to SPI and only input needed for this is monthly streamflow data. In previous research, streamflow data have been widely used for hydrological drought analysis (Dracup et al., 1980; Van Loon and Laaha, 2015; Kazemzadeh and Malekian, 2016; Kubiak-Wójcicka and Bąk, 2018). The reasons for selecting these three drought indices (SPI, EDI, SSFI) are (i) SPI is the most used index for drought monitoring around the world (Kchouk et al., 2022; Yildirim et al., 2022); (ii) WMO recommended to use SPI for drought monitoring (World Meteorological Organization, 2012); (iii) EDI is popular and preferable for arid/semi-arid regions (Dogan et al., 2012; Kamruzzaman et al., 2019; Malik et al., 2021; Mondol et al., 2021); (iv) EDI and SPI have similarities and hence can be used together for drought monitoring (Adisa et al., 2021); (v) Decile, which is used by The Bureau of Meteorology for drought monitoring in Australia, is not able to detect drought onset and end (Kanellou et al., 2008); and (vi) SSFI has not been used in Australia for hydrological drought monitoring (Yildirim et al., 2022).

A rank-based non-parametric method, Mann-Kendall (MK) test (Mann, 1945; Kendall, 1975), is commonly applied to perform trends in hydrology (Helsel and Hirsch, 1992; Zhang et al., 2001; Yilmaz and Perera, 2015; Kocsis et al., 2017; Jehanzaib et al., 2020a). In this study, however, we used the modified MK (M-MK) (Hamed and Rao, 1998) test to reduce the effect of serial correlation on the MK test results. Identification of change points in annual streamflow time series has been widely used in hydrological drought studies (Jehanzaib et al., 2020a, 2020b; Shah et al., 2022). Step changes in annual streamflow were detected by Pettitt test (Pettitt, 1979). Pearson's correlation (Pearson, 1895) and Spearman's rank correlation (Spearman, 1904) were applied here to assess correlation between meteorological and hydrological drought indices for different timesteps. The theory of run (or run theory) (Yevjevich, 1967) was applied here to detect drought propagation time from meteorological to hydrological drought (Wu et al., 2021). The maps and spatial interpolations were made using ArcGIS 10.6.1.

In previous studies, detailed drought hazard and comprehensive analysis covering both meteorological and hydrological droughts in Australia are lacking. Kiem et al. (2016) noted three key challenges in a drought study, which focus on drought hazard to improve understanding and management of Australian droughts. Therefore, we aim to fill the currently existing knowledge gap in drought science by investigating drought hazard, frequency, and propagation (from meteorological to hydrological drought) in southeast Australia by using long-term monthly rainfall and streamflow dataset.Overall, the aim of this study is to investigate the spatio-temporal characteristics of meteorological and hydrological droughts in southeast Australia. The objectives of this study therefore are (1) to apply a conceptual model to assess meteorological drought hazard; (2) to estimate frequency of drought and map it through a spatial

interpolation method; (3) to analyze trends in long-term streamflow data and to identify abrupt changes before and after the break points, if any; (4) to depict trends in hydrological droughts; (5) to assess correlation between meteorological (SPI, EDI) and hydrological (SSFI) drought indices for different timesteps; and (6) to identify when a meteorological drought becomes a hydrological one and discuss the possible factors that potentially affect the propagation time.

2. Study area and data

The study selected southeast Australia as the study area. This has an area of 1,028,790 km^2 covering the most populous states of New South Wales (NSW) and Victoria (VIC) (Fig. 1). Three main national catchments, Murray-Darling Basin (MDB), Lake Eyre Basin (LEB), and South East Coast (SEC) are located in the study area. The MDB is the twentieth largest river catchment in the world, which contains twenty-two major catchments covering most of inland of NSW and north of VIC. SEC lies east of MDB and covers most of coastal NSW and VIC. The study area accounts for approximately 63% of water quantity in Australia, and roughly 98% of water sources comes from surface water. Southeast Australia is located in arid, semi-arid and temperate climate zone (Bureau of Meteorology, 2016) with average annual rainfall increasing from northwest to southeast.

Monthly rainfall data from 104 stations (between 1858 and 2019), shown in Fig. 1a, were obtained from Australian Bureau of Meteorology (Bureau of Meteorology, 2020a). Statistics on monthly rainfall data were calculated: record lengths were more than 100 years for 97 stations, average length of 123 years, minimum length of 81 years, the median data length of 122.5 years. These rainfall stations are located across 45 rainfall districts in south-east Australia, with at least 2 rainfall stations from each rainfall district. In contrast to rainfall data, streamflow gauges had less data length. We, however, aimed to choose relatively long periods of streamflow records (greater than 40 years), stations being spatially distributed with fewer missing data. Finally, monthly streamflow data from 49 stations covering 1948–2019 were obtained, as shown in Fig. 1b (DELWP, 2020; WaterNSW, 2020).

3. Methodology

In this study, we carried out a spatiotemporal analysis of meteorological and hydrological droughts to characterize the nature of droughts in southeast Australia. Major parts of the adopted analytical framework can be stepped out as below: (1) Meteorological drought hazard and frequency analyses were undertaken by using SPI and EDI from monthly rainfall data; (2) Monotonic trends of streamflow with their step changes and hydrological droughts were found using the M-MK test, Sen's slope estimator and the Pettitt

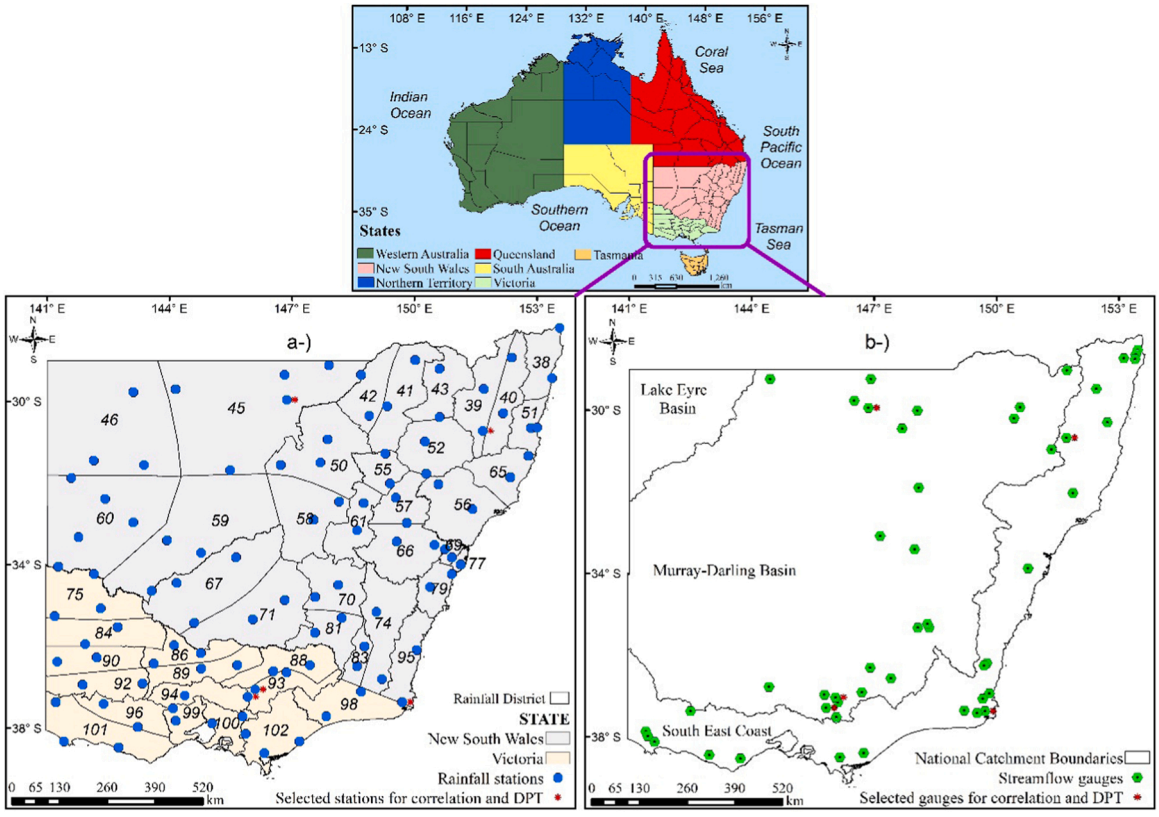

Fig. 1. Map of study area with well-distributed (a) rainfall stations and (b) streamflow gauges. Selected stations were used in Pearson's and Spearman's rank correlation, and drought propagation time (DPT) analyses.

test; (3) The hydrological drought frequency was estimated using SSFI from monthly streamflow discharge records; (4) Correlation between SPI/EDI and SSFI were assessed by Pearson's and Spearman's rank correlations; and (5) Estimation of drought propagation time (DPT) from meteorological to hydrological drought was done using 'theory of run.' The framework of the methodology for this study is given in Fig. 2.

3.1. Meteorological and hydrological drought identification using theory of run

A time series analysis method called, 'run theory', was introduced by Yevjevich (1967) to identify hydrological drought characteristics and to investigate their statistical properties, such as intensity, magnitude, and duration. The theory of run to characterize drought events for a given threshold is illustrated in Fig. 3. A 'run' is explained as part of time series of drought parameter X_t, in that all values are either under or over the selected threshold X_0, accordingly referred to as a 'negative run' or a 'positive run', respectively (Mishra et al., 2009; Mishra and Singh, 2010). Drought identification concept (Fig. 3), which was pro-adopted by Yevjevich (1967) and Dracup et al. (1980) can be described as follows: A drought starts any time when X_t (X_t refers to EDI, SPI, or SSFI in this case) is continuously less than zero (X_0) and achieves an intensity of − 1.0 or less. Drought terminates when X_t is positive. The duration (or run-length) is defined as the period of time between drought initiation (t_i) and termination time (t_e). The magnitude (or run-sum) is the accumulated water deficit (e.g. rainfall) during the drought. Intensity (or run-intensity) is calculated as the drought magnitude divided by its duration.

Drought classifications based on EDI, SPI, and SSFI are shown in Table 1 (McKee et al., 1993; Hayes et al., 1999; Modarres, 2007; Dogan et al., 2012). The details of EDI, SPI and SSFI are explained in detail in Appendix A.

3.2. Drought hazard and frequency analyses

3.2.1. Drought hazard index

Drought severity and occurrence probability were used to quantify drought hazard by assigning weights and ratings based on the cumulative distribution function (Fig. 4). The occurrences of drought were examined, based on the frequencies of drought events for each drought class for multiple timesteps. Sönmez et al. (2005) explained the percentages of drought occurrence as the ratio of drought occurrences in each time step to the total drought occurrences in the same drought category and timestep. In this study, the drought occurrence probabilities were calculated for all the selected stations for EDI and SPI of multi-timesteps in southeast Australia.

The Drought Hazard Index (DHI) concept was applied to address drought hazard in this study. DHI was calculated as below. First of all, the weights, varying from 1 to 4, were assigned according to Table 1, and secondly the ratings were assigned from 1 to 4 by evenly dividing the range of drought occurrence probability according to Fig. 4. Thiessen polygon (Thiessen, 1911) was used to find areal ratio of each station and average weight (ratio) calculated based on each station for each district. Lastly, DHI was integrated by using the weights and the ratings as below (Kim et al., 2013):

$$DHI = (NND_w \times NND_r) + (MD_w \times MD_r) + (SD_w \times SD_r) + (ED_w \times ED_r) \quad (1)$$

where w and r refer to weight and rating, respectively. The maximum and minimum values of DHI would be 40 and 10, respectively. DHI, however, must be normalized from 10 to 40–0–1. Therefore, DHI was re-scaled using the normalization method as below:

$$nv_i = \frac{v_i - v_{min}}{v_{max} - v_{min}} \quad (2)$$

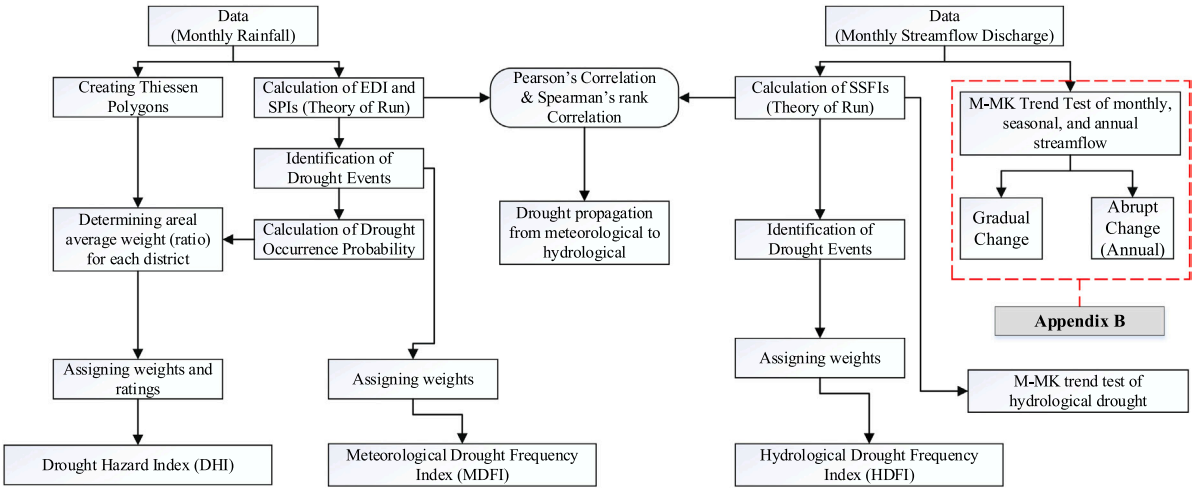

Fig. 2. Framework for assessing drought hazard, frequency and drought propagation time.

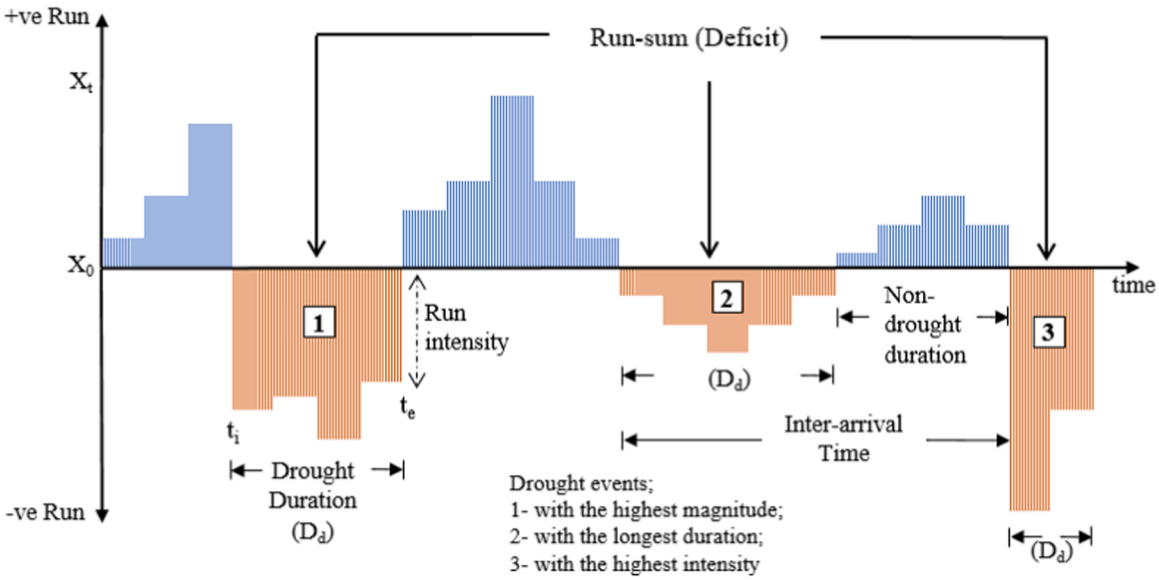

Fig. 3. Concept of run theory for a given threshold level.

Table 1
Drought classification scales for EDI, SPI and SSFI values.

Drought Index	Extreme Drought (ED) (4)**	Severe Drought (SD) (3)	Moderate Drought (MD) (2)	Near Normal Drought (NND) (1)
EDI	≤ −2.00	(−1.99) - (−1.50)	(−1.49) – (−1.00)	(−0.99) – (0.99)
SPI	≤ −2.00	(−1.99) - (−1.50)	(−1.49) – (−1.00)	(−0.99) – (0.99)
SSFI	≤ −2.00	(−1.99) - (−1.50)	(−1.49) – (−1.00)	(−0.99) – (0.99)

*Wet conditions are not shown.
** Numbers in parenthesis under drought classes, from 1 to 4, refer to weights for DHI and DFI.

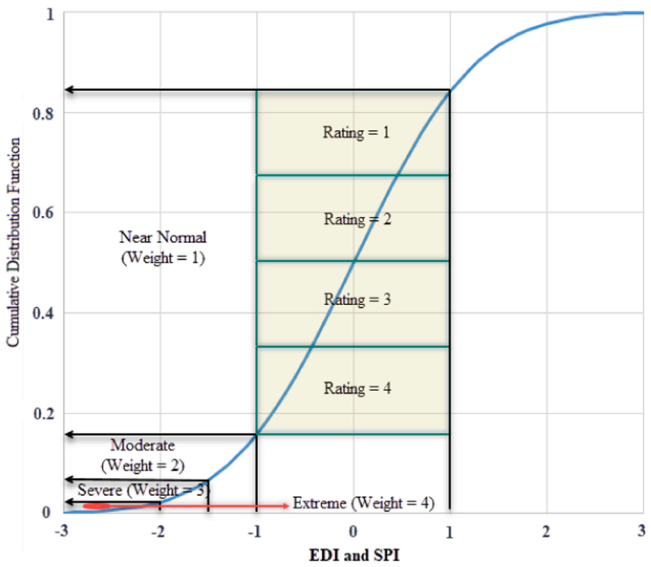

Fig. 4. Weight and rating scores based on the cumulative distribution function of EDI and SPI.

where v_{min} and v_{max} are the minimum and maximum values for variable v, and nv_i is the normalized value. Then, DHI was classified into four classes as shown in Table 2.

3.2.2. Drought frequency index

Drought frequency analysis addressed to monitor short term and long term either meteorological or hydrological drought vulnerability in southeast Australia. For this goal, Drought Frequency Index (DFI) (Eslamian and Eslamian, 2017) was calculated to detect vulnerable districts and streams in southeast Australia. DFI was calculated as below:

$$DFI = \frac{NND_w \times NND_n + MD_w \times MD_n + SD_w \times SD_n + ED_w \times ED_n}{4D_l} \tag{3}$$

where w and n present the weights and number of occurrences of particular drought, respectively. D_l is the data length of a given station. In this way, maximum weighted drought frequency index value would be 1, and the minimum value would become 0 (drought-free). Then, DFI was classified into four classes as illustrated in Table 3.

3.3. Trend and step change analyses

Investigation of annual streamflow data series and trend analysis were performed in this study. Monotonic trends can occur either abruptly or gradually in streamflow data. For this purpose, modified (Hamed and Rao, 1998) non-parametric Mann-Kendall test (Mann, 1945; Kendall, 1975) was used to detect monotonic trends in annual streamflow data and Sen's slope estimator (Sen, 1968) was applied to calculate the magnitude of trend. Pettitt Test (Pettitt, 1979) was used to detect step change in the time series of streamflow data for all selected gauging stations. Pettitt test detects one single change point, and it is more susceptible to find abrupt change in the middle of time series (Hawkins, 1977; Wijngaard et al., 2003; Costa and Soares, 2009). The details of M-MK, Sen's slope estimator, and Pettitt test are explained in Appendix A.

3.4. Drought propagation time

Drought propagation time (DPT) from meteorological to hydrological drought can be defined as the difference between the onset of hydrological drought and that of meteorological drought (Edossa et al., 2010; Zhao et al., 2019; Wu et al., 2021). DPT was identified by run theory as below:

$$DPT = \frac{\sum_{i}^{N} (O^i_{HD} - O^i_{MD})}{N} \tag{4}$$

where O^i_{HD} and O^i_{MD} represent the onset of hydrological and meteorological droughts, respectively, and N is the number of drought events. Finally, DPT is obtained as month since the SPI and SSFI were taken on the month scale.

4. Results and discussion

4.1. Meteorological drought assessment

4.1.1. Assessment of meteorological drought hazard

Since DHI provides regional drought hazard considering drought severity and occurrence probability, we created a DHI map at the rainfall district level based on EDI and multi-timestep-SPI to assess the spatial distribution of meteorological drought hazard. The drought occurrence probabilities in this study were calculated for each of the selected stations based on EDI and six different timesteps-SPI (3-, 6-, 9-, 12-, 24-, 36-month) and summarized the results for five rainfall stations in Table 4.

As an illustration, RD-69, located in NSW has the Thiessen polygons consisting of five rainfall stations (68045, 69018, 69029, 70009 and 70045), with ratios of 5.5%, 56.6%, 19.8%, 17.2%, and 0.9%, respectively. We should note that not all these five stations are within RD-69, and the Thiessen polygons (voronoi diagrams) of these five stations are also located in RD-69.

These five stations' drought occurrence probabilities (DOP) of moderate drought (MD) were 6.7%, 9.5%, 9.1%, 8%, and 10.8%, respectively (Table 4). Therefore, areal weighted probability of drought occurrence for RD-69 was found as 9% ($=0.055 \times 6.7 + 0.566 \times 9.5 + 0.198 \times 9.1 + 0.172 \times 8 + 0.009 \times 10.8$). Similarly, areal weighted DOP of NND, SD, and ED were

Table 2
DHI classification scheme by range (Kim et al., 2013).

DHI range	DHI classes
$0 \leq DHI < 0.25$	Low
$0.25 \leq DHI < 0.50$	Moderate
$0.50 \leq DHI < 0.75$	High
$0.75 \leq DHI < 1.0$	Very High

Table 3
Weighted classification scheme for DFI (Eslamian and Eslamian, 2017).

DFI range	Drought frequency classes
$0 < DFI \leq 0.20$	Low
$0.20 < DFI \leq 0.40$	Moderate
$0.40 < DFI \leq 0.60$	High
$0.60 < DFI \leq 1.00$	Very High

Table 4
Meteorological drought occurrence probability (%) based on EDI in rainfall district-69 (RD-69).

ID	Station Name	State	Wet	NND	MD	SD	ED
68045	Moss Vale	NSW	40.8	48	6.7	3.2	1.3
69018	Moruya Heads	NSW	35.5	47.6	9.5	5.2	2.3
69029	Eden	NSW	37.3	47.4	9.1	4.9	1.3
70009	Bukalong	NSW	38.6	49	8	3.9	0.6
70045	Hall	NSW	34	48.6	10.8	5.9	0.7

*NND: Near normal drought; MD: Moderate drought; SD: Severe drought; ED: Extreme drought

Table 5
Weights and ratings of drought severity for EDI (DHI).

Severity	Weight	Drought Occurrence Probability (DOP) (%)	Rating
Near Normal	1	$DOP < 47.00$	4
		$47.00 \leq DOP < 47.85$	3
		$47.85 \leq DOP < 48.69$	2
		$48.69 \leq DOP < 49.54$	1
Moderate	2	$DOP < 7.64$	4
		$7.64 \leq DOP < 9.16$	3
		$9.16 \leq DOP < 10.68$	2
		$10.68 \leq DOP < 12.20$	1
Severe	3	$DOP < 3.32$	4
		$3.32 \leq DOP < 4.47$	3
		$4.47 \leq DOP < 5.61$	2
		$5.61 \leq DOP < 6.75$	1
Extreme	4	$DOP < 1.57$	4
		$1.57 \leq DOP < 2.60$	3
		$2.60 \leq DOP < 3.64$	2
		$3.64 \leq DOP < 4.67$	1

calculated as 47.8%, 4.8%, and 1.7%, respectively. Weights and ratings of RD-69 were selected from Table 5 (ratings were assigned by dividing the range into 4, as explained in Fig. 4). For example, the weight of MD was "2" and the rating of MD for RD-69 was "3" (Table 5). Weights and ratings for the other drought categories (NND, SD, and ED) assigned in the similar way. Then, DHI was calculated as 27 (from equation 1), which was a relatively high value compared to other districts, and was re-scaled to 0.57 (from equation 2). Finally, RD-69 was classified as "High" for DHI = 0.57 (see Table 2). The same procedure was applied to all the stations and districts, then ultimate 'DHI spatial map' was created for EDI and multi-timestep-SPI as shown in Fig. 5.

Fig. 5 depicts the spatial DHI in southeast Australia and it shows that EDI and all timestep-SPIs have detected "Very High" level DHI at least in one district. It is clear that there was no low DHI based on short term drought and seasonal drought, which were 3-, 6-, 9-month SPIs (Fig. 5a, b, and c). Furthermore, 67% of the districts had "High" level DHI based on 3-month SPI. The south of the study area was detected as the most drought prone part based on the 6-month SPI, which indicates seasonal to medium term trends. The 9-month SPI was dominated by a "Moderate" DHI in the region, and 69% of the districts were categorized as having moderate drought hazard level, and the south-east coast of the region mainly faced a "High" level drought. Two rainfall districts, RD-87 and RD-61 were found to have a "Very High" level DHI based on 3-, 6-, and 9- month SPI. Although two districts (RD-47 and RD-75) had "Low" DHI, south and south-east coastal areas were dominated by "High" and "Very High" DHI levels based on 12-month SPI (Fig. 5d). The maximum numbers of "Very High" level DHI were detected, based on 24-month SPI (long term drought) in south of the study area. A big portion of the north-east of NSW was dominated by "High" and "Very High" levels of DHI in terms of 24-month SPI. Similar to other long-term drought indicators, 36-month SPI was detected as "High" and "Very High" level DHI mainly in the south of the study area. EDI was detected as "Very High" and "High" level DHI in the region at three and twenty-two districts, respectively. EDI, interestingly, was found to be the only index with three "Low" DHI in the inner northwest of NSW. Victoria was found to be the most drought prone area by EDI with 12 districts having either "High" or "Very High" levels of DHI and other three districts were found to have "Moderate" level DHI. "Moderate" DHI was detected for RD-76 and RD-82 for all timestep-SPI. Besides, RD-85, RD-86 and RD-87 were found to be extremely drought prone, having "High" level (or "Very High" level) DHI for all timestep-SPI. Other rainfall districts, RD-88, RD-89,

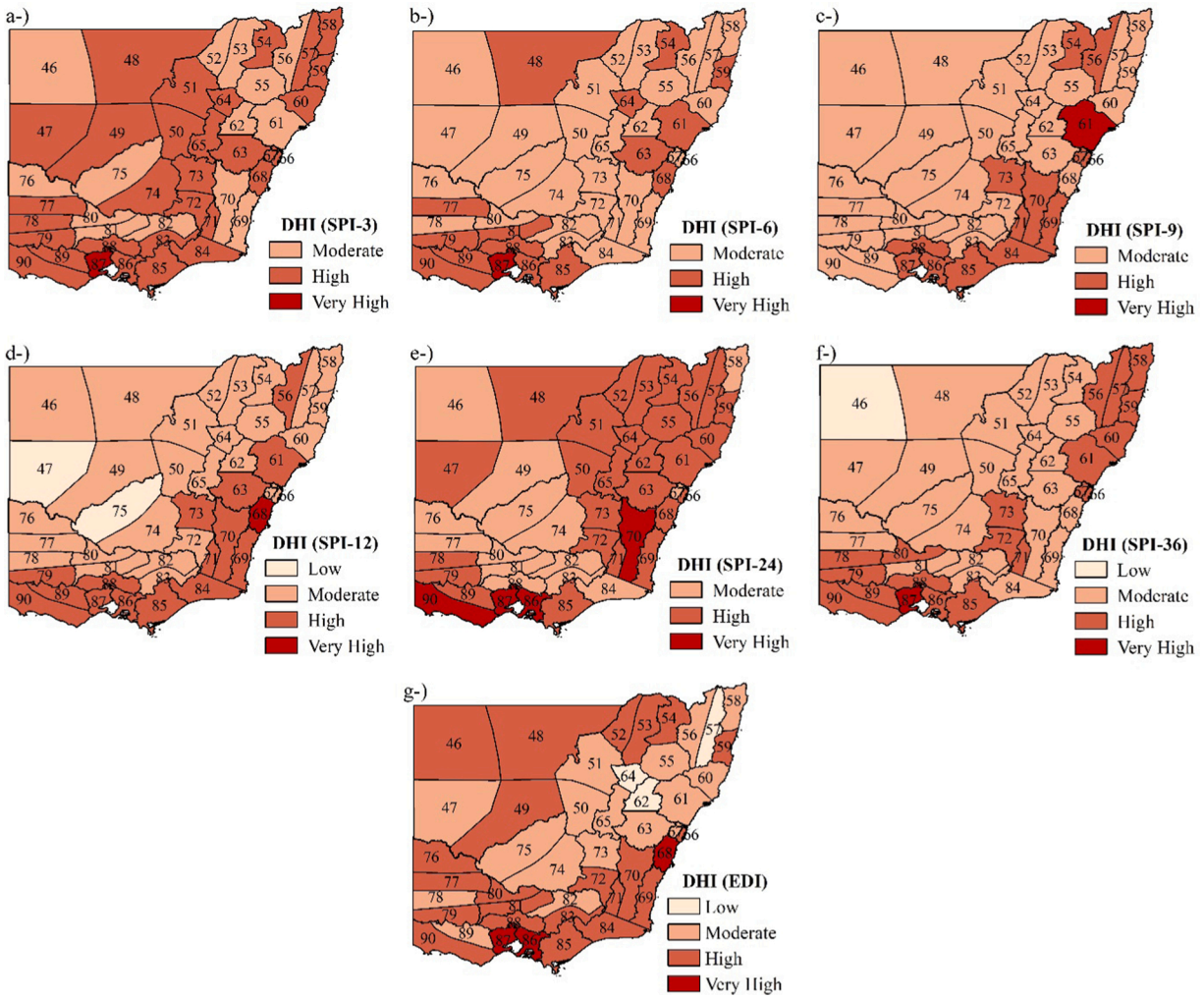

Fig. 5. DHI map for EDI and multi-timestep-SPI in southeast Australia. ("*n*" refers to the month in SPI-n, e.g., 3-month SPI is shown as SPI-3).

and RD-90 were also drought prone districts with mainly "High" or "Very High" level DHI.

Fig. 6 illustrates the distribution of districts based on different DHI classes. 30 rainfall districts out of 45 were found having "High" level drought hazard based on 3-month SPI, and this is the worst case compared to other SPIs and EDI. The numbers of districts having "High" level DHI by 3-month, 24-month SPI and EDI were higher than those having "Moderate" DHI in the study area.

The areal coverage of DHI is presented in Table C1. For instance, the areal coverage of "Low", "Moderate", "High", and "Very High" DHI (based on EDI) were 3.9%, 39.6%, 54.1%, and 2.5%, respectively. The areal coverage of "High" level DHI was found as 64.4%, 57.1%, and 54.1% of the south-eastern Australia based on 3-month (short term) and 24-month (long term) SPI, and EDI, respectively.

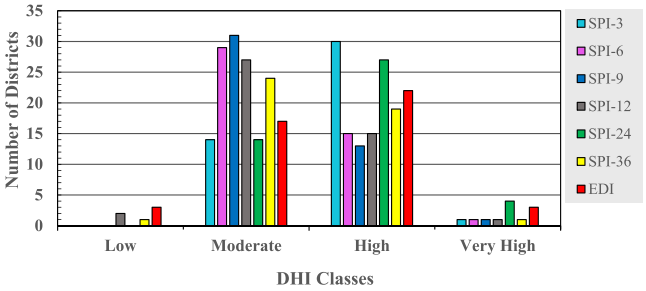

Fig. 6. DHI found by EDI and multi-timestep SPI at the district level in southeast Australia.

4.1.2. Assessment of meteorological drought frequency

Drought frequency analysis is vital for drought vulnerability assessment. Frequencies of different drought categories can be mapped through spatial interpolation of data points to demarcate various drought-prone zones. Here, we investigated drought frequency by assigning proper weights, calculating the number of drought event, and considering data length of each of the selected rainfall stations. Finally, meteorological drought frequency index (MDFI) was calculated for all the stations and interpolated by using the spline interpolation technique (Talmi and Gilat, 1977; Hartkamp et al., 1999) in ArcGIS environment (Fig. 7).

Fig. 7 clearly shows that frequency (for SPI) is changing with time. The duration of droughts based on SPI increases, whereas the frequency decreases and vice versa (McKee et al., 1993). EDI detected "High" level drought frequency mainly in east and south-west of the study area, while north-west of the study area experienced "Moderate" level MDFI. "Low" level MDFI was not detected for EDI for any rainfall station, whereas 12- and 24-month SPI had low level MDFI in terms of all other timesteps-SPI. "Very High" level MDFI was computed at 3-month accumulation period at all rainfall stations. This result shows similarities with DHI at 3-month SPI. "High" level MDFI was found in the east and south coastal areas, which have vital importance in terms of hydrological drought as well, since high frequency of meteorological drought increases the occurrence probability of hydrological drought. Spinoni et al. (2014) studied drought frequency and severity in a global scale by using 12-month SPI with data covering 1951–2010 and they found significant increasing frequency in southeast Australia. South-west of the study area, which is winter dominant (wet winter and low summer rainfall) climate zone, experienced higher MDFI for SPI and EDI of each time steps. This outcome reveals the importance of seasonal rainfall on drought frequency analysis.

4.1.3. Regional assessment of meteorological drought

The study area was divided into three-hydrological regions, based on annual average rainfall (AAR) distribution by using the Jenks natural optimization method (Jenks, 1967). The Jenks optimization method seeks to minimize each class's mean deviation from the class average, whereas maximizing each class's deviation from the mean of the groups. Therefore, the method seeks to reduce the

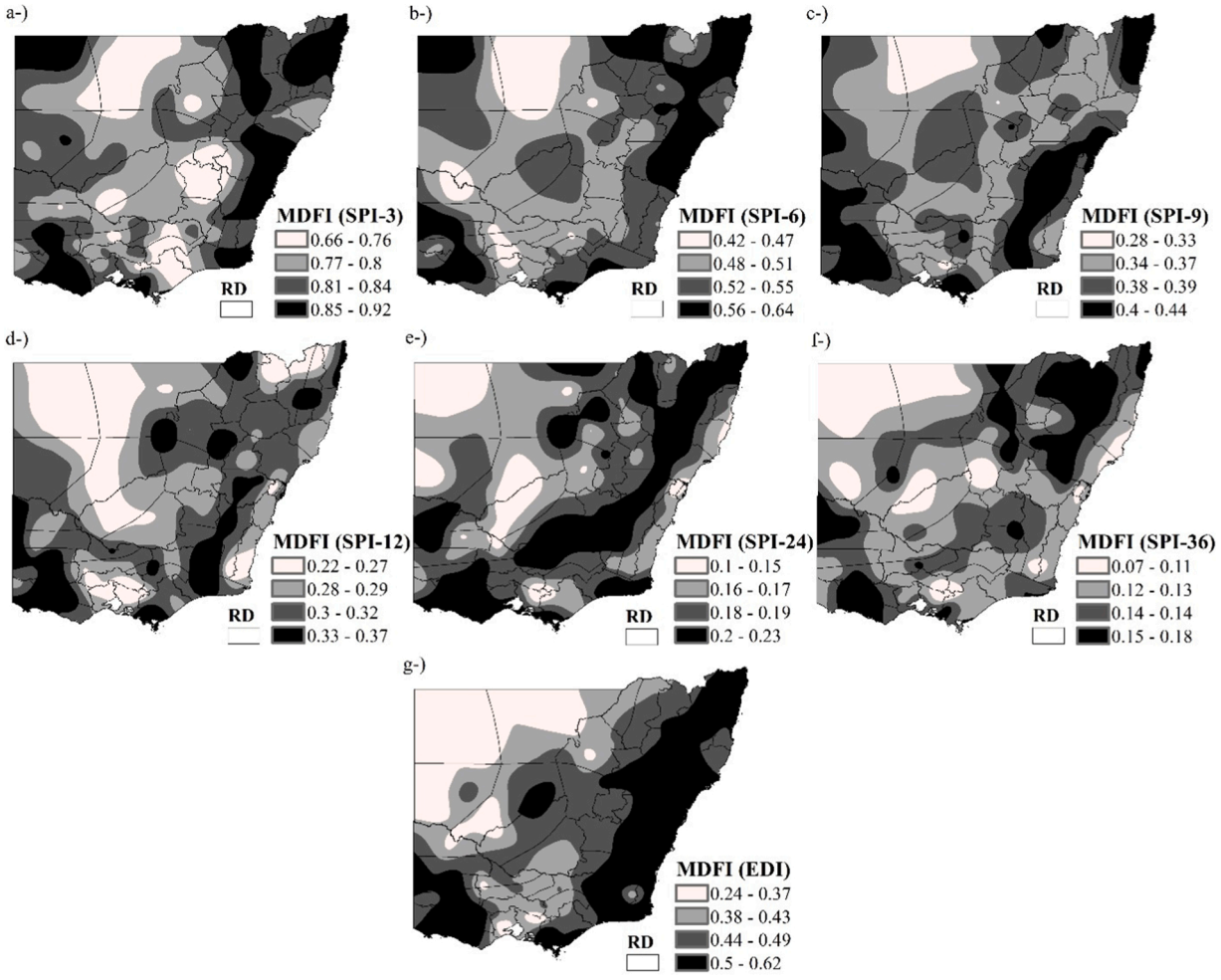

Fig. 7. Weighted meteorological drought frequency index (MDFI) for EDI and SPI of multi-time steps in southeast Australia ("*n*" refers to month in SPI-n, e.g., 9-month SPI is labeled as SPI-9 and RD refers to Rainfall District).

variance within classes and maximize the variance between classes. What's more, our hydrological divisions (Fig. 8a) show high similarity with Köppen climate classification (Bureau of Meteorology, 2016) which is essential for the accuracy of regional drought assessment.

Climatic features of divisions are as follows: Region-1 is regarded as "arid", Region-2 is "semi-arid", and Region-3 is "temperate" climatic zone. The numbers of rainfall stations for each region were 11, 32, and 59, respectively. Besides, regional drought occurrence probability based on EDI and different timestep-SPIs are shown in Fig. 8b. The maximum total (ED + SD + MD) drought probabilities were calculated at 3-month SPI for all regions; here the minimum one was detected by EDI for Region-1 and Region-2. The highest extreme drought probabilities in Region-1, Region-2, and Region-3 were detected by SPI-3 as 7.2%, 7.1%, and 6.4%, respectively. Furthermore, considering long term droughts (e.g. 12-, 24-, and 36-month SPI), SPI-12 detected the maximum total drought occurrence probabilities in each region. Shukla and Wood (2008) found that SPI-12 and standardized runoff index (SRI), used for hydrological drought monitoring, were similar and had high correlation to depict hydrological aspects of droughts. Wasko et al. (2021) reported decreasing rainfall between 1960 and 2017 in the southeast of Australia causing a prolonged period of drought. Gallant et al. (2013) found that the number of drought events in southeast of Australia had statistically decreasing trend and increasing average duration over the period 1960–2009.

The MDFI distribution at the regional scale is shown in Fig. 9. Region-3, which has the highest AAR considering the whole study area, had the topmost MDFI level for all the timesteps- SPI and EDI compared to Region-1 and Region-2. This result is of vital importance in terms of the likelihood of hydrological drought in the region as well. As it is seen from Fig. 9, the frequency of meteorological drought is decreasing as timesteps of SPI are increasing. EDI which is a time-independent drought index detected "High" level MDFI in Region-2 and Region-3.

4.2. Historical trends of streamflow

A set of 13 gauging stations was identified with step change in annual total streamflow at 0.01 significance level (Table 6). Table 6 shows that the majority of stations showed an abrupt change in the mid-90 s and early-00 s when one of the worst historical droughts hit (Van Dijk et al., 2013) southern and eastern parts of Australia (Murphy and Timbal, 2008), the so-called "millennium drought" (Bond et al., 2008). The most dominant year of step change was found to be 1996 for 7 out of 13 stations. Zhang et al. (2016) studied changes in total annual streamflow across Australia and detected the step change by the distribution-free CUSUM method. Similar to our study, they found significant decreasing trends in annual streamflow in NSW and VIC. Besides, our results of abrupt change showed similarity with this study. In addition, we investigated monotonic trends before and after the break year (Salarijazi et al., 2012) differently from Zhang et al. (2016) (Table 6). Out of 13 stations, only 3 showed an increasing trend before and after the step change, although these stations had gradual decreasing trends in the long-term using the M-MK test and Sen's slope. Upward trends were determined for 8 out of 13 stations after the abrupt change. Spatial variations of annual total streamflow with directions and step

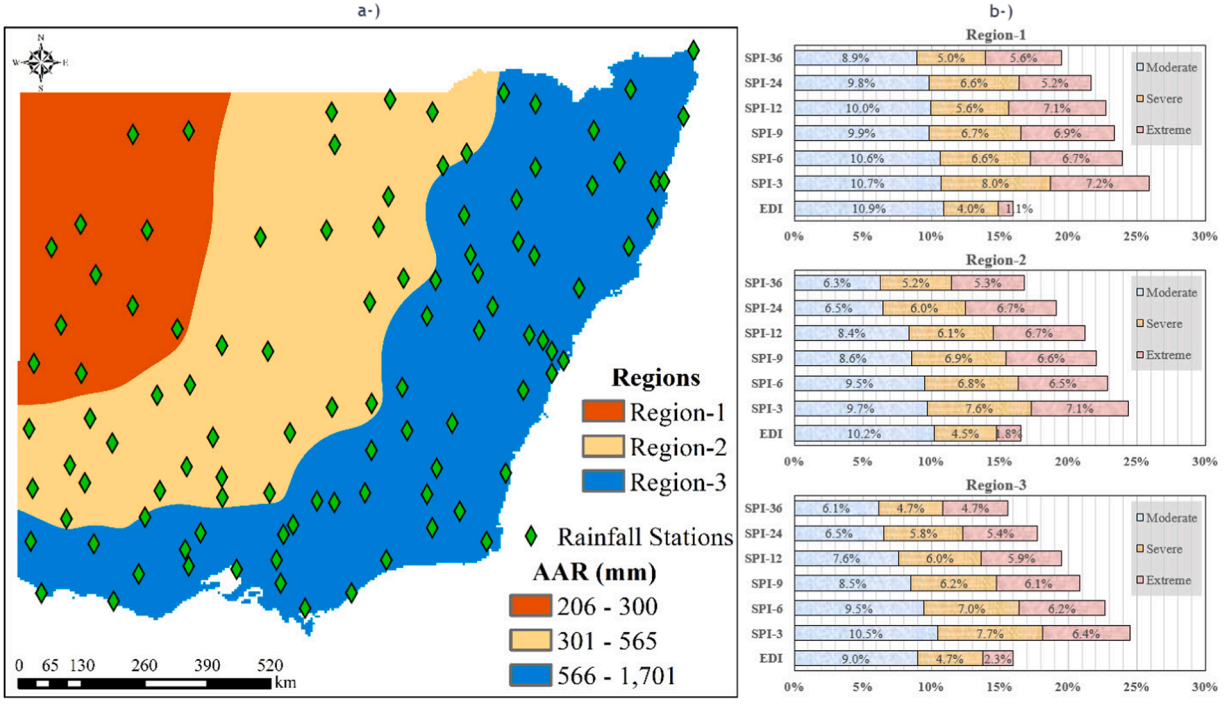

Fig. 8. Hydrological divisions and their drought occurrence probabilities based on EDI and SPI.

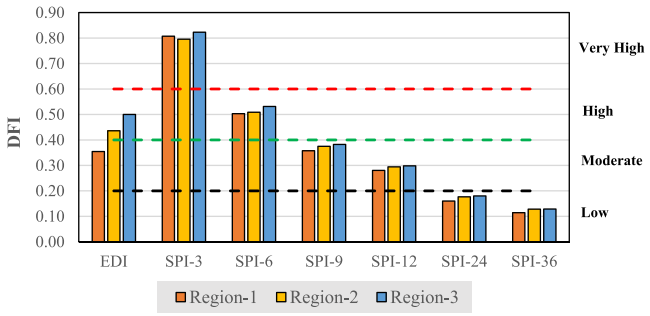

Fig. 9. Hydrological divisions and their frequency distribution based on EDI and SPI.

Table 6
Results of M-MK trend test, Sen's slope estimator and step (abrupt) change by Pettitt test.

Station ID	Site name	Basin	Catchment Area (km^2)	State	Data Time series (year)		Ave. Annual flow (GL/yr)	Trend		Abrupt Change**
					Start	End		Kendall's tau	Sen's Slope	
202001	Brunswick River at Durrumbul	Brunswick River	34	NSW	1972	2019	24.4	-0.222	-0.347	(↓)1990 (↑)
227210	Bruthen Creek at Carrajung Lower	South Gippsland	18	VIC	1953	2019	4.0	-0.460*	-0.089	(↓)1996 (↓)
233214	Barwon River East Branch at Forrest	Barwon	17	VIC	1956	2019	7.5	-0.261*	-0.078	(↑)1996 (↑)
237202	Fitzroy River at Heywood	Portland Coast	234	VIC	1969	2019	26.7	-0.241	-0.426	(↓)1992 (↑)
238207	Wannon River at Jimmy Creek	Glenelg	40	VIC	1953	2019	9.6	-0.437*	-0.175	(↓)1996 (↓)
238230	Stokes River at Teakettle	Glenelg	181	VIC	1975	2019	14.3	-0.240	-0.277	(↓)1996 (↑)
238235	Crawford River at Lower Crawford	Glenelg	606	VIC	1971	2019	42.1	-0.299*	-0.817	(↓)1992 (↑)
405245	Ford Creek at Mansfield	Goulbrun	115	VIC	1971	2019	9.9	-0.279*	-0.208	(↑)1996 (↓)
405251	Brankeet Creek at Ancona	Goulbrun	121	VIC	1974	2019	13.8	-0.360*	-0.324	(↑)1996 (↓)
406214	Axe Creek at Longlea	Campaspe	234	VIC	1973	2019	12.2	-0.373*	-0.381	(↓)1996 (↓)
410061	Adelong Creek at Batlow Road	Murrumbidgee River	144	NSW	1948	2019	36.5	-0.300*	-0.403	(↓)2000 (↑)
412004	Lachlan River at Forbes	Lachlan River	19,000	NSW	1976	2019	873.8	-0.247	-14.680	(↑)2001 (↑)
412006	Lachlan River at Condobolin Bridge	Lachlan River	25,200	NSW	1965	2019	694.0	-0.187	-5.896	(↑)2002 (↑)

* Indicates significant trends at $p < 0.01$
** Abrupt change at significance level of 0.01. Arrows in left and right sides of abrupt change show the trends before and after the break year, respectively.

changes at different significance levels (0.01, 0.05, 0.10) are shown in Fig. 10. Although all streamflow stations showed a decreasing trend (when significance level was ignored) (Table B1), statistically significant decreasing trends and decreasing step change were detected mainly in the south of the study area (Fig. 10). This finding is consistent with Zhang et al. (2016) and (Wasko et al., 2021). Very strong evidence for decreasing trend, based on annual total streamflow, was detected at the significance level of 0.01 in the south of Southeast Coast (SEC)/Murray Darling Basin (MDB) and north of MDB. Streamflow trend analysis, covering monthly and seasonal average flows, are explained in detail in Appendix B. Dai (2021) investigated global hydro-climatic trends during 1950 and 2018 and noted that rainfall and streamflow had decreased in eastern Australia, which supports our findings. Furthermore, decreasing streamflow trends in our study showed high similarities with Wasko et al. (2021).

4.3. Hydrological drought assessment

In order to understand hydrological aspects for adequate drought management, hydrological drought was quantified by using SSFI to identify drought characteristics such as drought onset-end, duration, magnitude, and intensity. Thereafter, hydrological drought events, occurrence of probability, hydrological drought frequency index (HDFI), and long-term trends (M-MK test) in multi-timestep

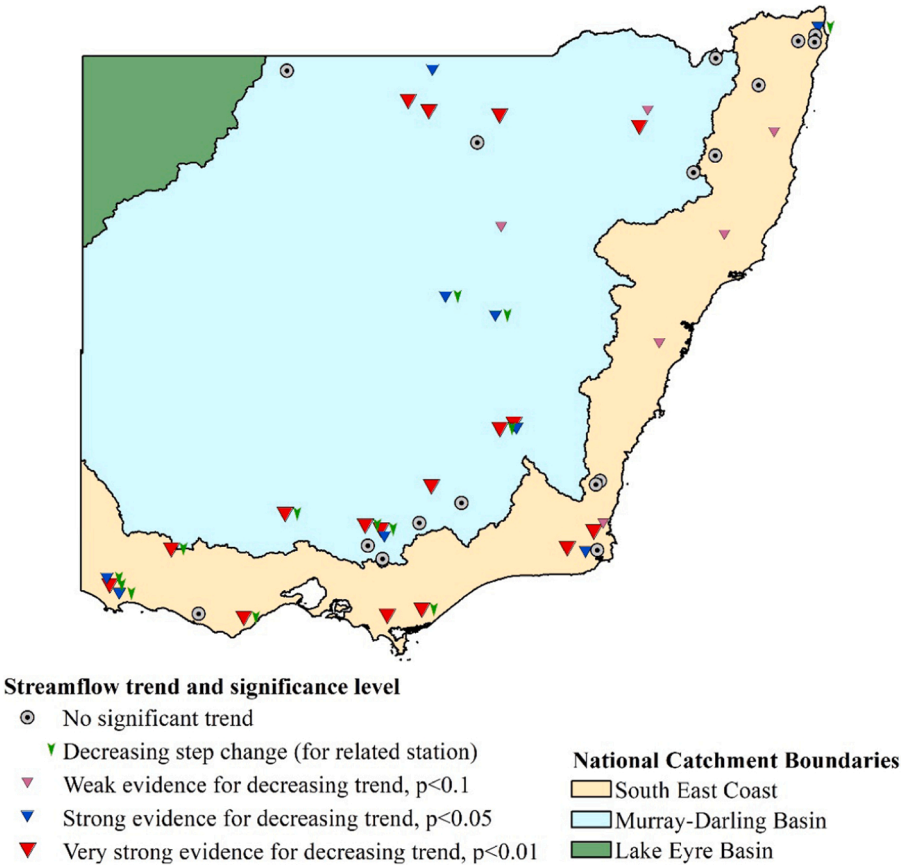

Fig. 10. Spatial distribution of M-MK trend analysis in annual total streamflow. Trends were shown in 0.01, 0.05, and 0.1 significance level.

SSFI were determined.

4.3.1. Trends in hydrological drought

Table 7 presents short- and long-term hydrological drought trends identified by M-MK test at significance levels of 0.01, 0.05, and 0.1. Results clearly showed that there was no significant upward trend in six different timesteps of SSFI at selected streamflow gauges.

Decreases in annual median streamflow in southeast Australia have been observed in the MDB and SEC (NSW and VIC). Downward trends in streamflow have been found between 50% and 75% of gauges in each of these basins since 1975. For example, more than 75% of the long-term streamflow gauges show a decreasing trend since 1970 (CSIRO and BOM, 2020) and our results for short- and long-term hydrological drought trends depict how these streamflow decreasing trends led to downward drought trends. Wasko et al. (2021) studied trends in simulated streamflow based on annual SRI across Australia and our findings support their results in southeast Australia.

4.3.2. Assessment of hydrological drought frequency

Fig. 11 illustrates hydrological drought frequency index (HDFI) from 3 to 36-month accumulation period in southeast Australia. As

Table 7
Number of streamflow gauges presenting positive and (negative) hydrological drought trends by the M-MK trend test for multi-timesteps of SSFI.

Hydrological Drought index	Significance Level ignored	Significance level considered		
		1%	5%	10%
SSFI-3*	0 (49)	0 (22)	0 (27)	0 (34)
SSFI-6	1 (48)	0 (22)	0 (30)	0 (35)
SSFI-9	0 (49)	0 (22)	0 (32)	0 (38)
SSFI-12	1 (48)	0 (24)	0 (35)	0 (38)
SSFI-24	2 (47)	0 (26)	0 (36)	0 (37)
SSFI-36	3 (46)	0 (23)	0 (34)	0 (36)

*n refers to months in SSFI-n (e.g. SSFI-6 is 6-month SSFI, SSFI-24 is 24-month SSFI and so on)

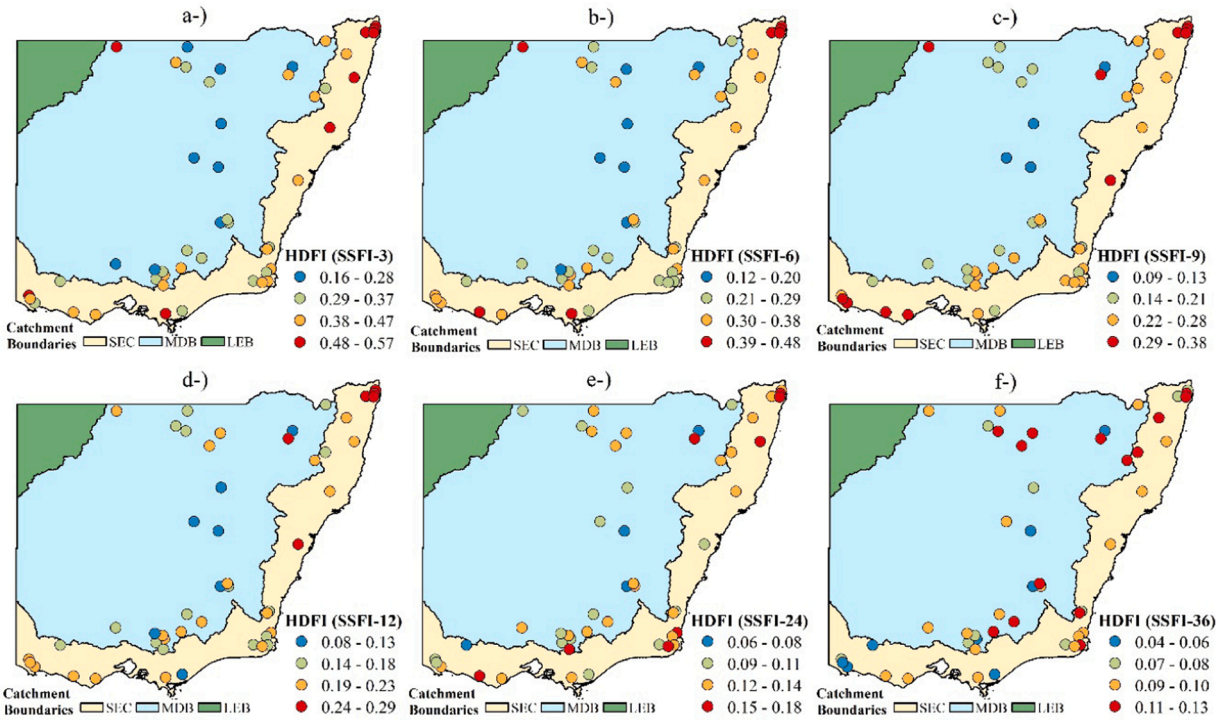

Fig. 11. Weighted hydrological drought frequency index (HDFI) for multi-timesteps SSFI in southeast Australia ("*n*" refers to month in SSFI-n, e.g. 3-month SSFI shown as SSFI-3).

expected, HDFI has been decreasing as a function of time whereas "High" level HDFI was determined at 3- and 6-month SSFIs. "Very High" level HDFI was not detected at any time step of SSFI. However, higher HDFIs for each timestep of SSFI were detected in SEC and north of MDB.

Furthermore, we also addressed changing of hydrological drought frequency and duration over the last decades. As given in Table 6, most of the step changes of streamflow were observed in the mid-1990 s, which is well known prolonged drought, "millennium drought" or "Big Dry" (Murphy and Timbal, 2008; Verdon-Kidd and Kiem, 2009) that affected southeast Australia. We,

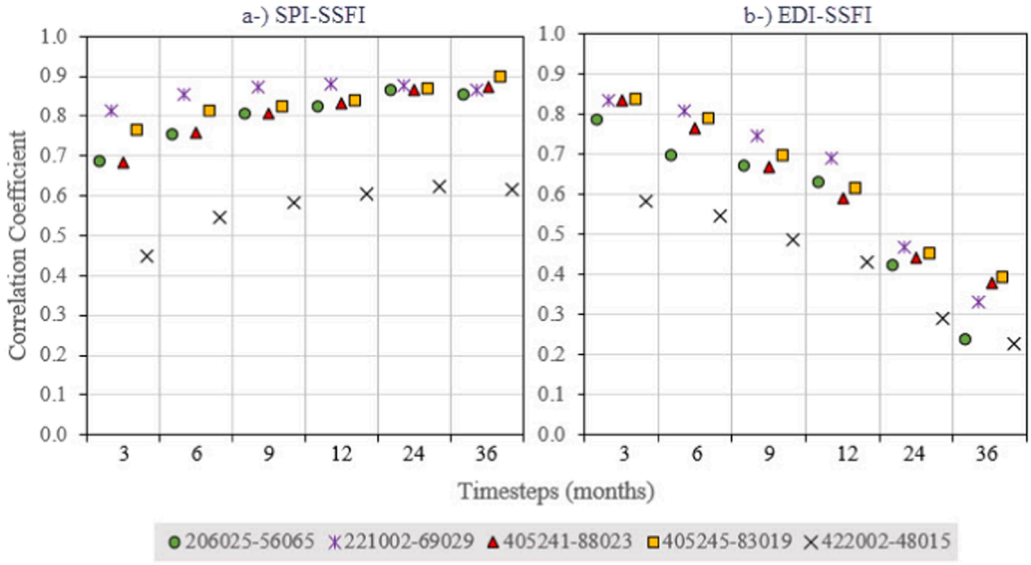

Fig. 12. Pearson correlation coefficients between (a) SPI-SSFI and (b) EDI-SSFI at different time-steps. Station IDs are represented as streamflow station-rainfall station. Correlation coefficient shows for e.g. 3-month SSFI-3-SPI-3, 6-month SSFI-6-SPI-6, and so on. (Note: EDI is timestep independent index).

therefore, compared the numbers of total drought (*Moderate* + *Severe* + *Extreme*) events before and after 1990 to depict changes in hydrological drought characteristics. For this goal, we selected nine streamflow gauges which had the longest (more than 60 years) data length to investigate changes in frequency and the results are summarized in Table C2. Average (standard deviation) results illustrated that 55% (±10%), 51% (±5%), 50% (±7%), 52% (±6%), 57% (±7%), and 66% (±16) of total droughts occurred after 1990 based on 3-, 6-, 9-, 12-, 24-, 36-month SSFIs, respectively. Similarly, longer hydrological drought duration in southeast Australia was experienced, based on the selected nine streamflow stations after 1990 (see Table C3).

Forootan et al. (2019) found that hydrological droughts in Australia between 2006 and 2011 were highly correlated with the IOD and the ENSO climate drivers where Wang et al. (2021) noted that the impact of IOD was stronger than El Nino on hydrological drought with comparison of 2006–2009 and 2018–2020 droughts. Besides, we know that four major climate drivers (SAM, ENSO, IOD, and IPO) influence droughts in south-eastern Australia (CSIRO, 2010). However, droughts characteristics due to climate drivers may not be similar in terms of magnitude, severity, spatial distribution, and so on (Verdon-Kidd and Kiem, 2009). Maximum hydrological drought quantities such as magnitude, duration, and intensity (severity) were detected mainly after 2000 at different accumulated periods and detected maximum hydrological drought quantities are listed in Table C4 with drought onset and end.

4.4. Comparison of meteorological and hydrological drought indices

The Pearson correlation coefficient was computed between drought indices at different timesteps (from 3- to 36-month) for better inter-comparison and to find the most appropriate accumulation period between SPI/EDI and SSFI. For this purpose, the closest five streamflow and rainfall stations were selected with average 5 km distance in order to apply correlation analysis (these are referred to as paired stations). Fig. 12a depicts correlation coefficient between SPI and SSFI at five paired stations. It is clear that the least correlation was detected at 3-month timestep ($0.45 < r_p < 0.82$) and the coefficient of correlation showed an increasing trend with time till 24-month accumulation period ($0.63 < r_p < 0.89$). After 24-month timestep, correlation coefficient was found to be increasing or decreasing at 36-month timestep. It should be noted that high correlation of 36-month accumulation period is not meaningful since, long-term calculation of SPIs (or SSFI) (longer than 24 month) fitting a distribution might be biased due to the limitation of data length (Mishra and Singh, 2010).

The correlation between the SPI and SSFI values at three different time steps (12-, 24-, 36- month) is depicted by drought severity time steps in Fig. C1 and scatter plots of these with confidence ellipse are shown in Fig. C2.

The least correlation coefficients at six different timesteps among five paired stations were found for 422002–48015 (streamflow gauge-rainfall gauge) ($0.45 < r_p < 0.63$) located in semi-arid climatic zone (Region-2). One of the main reasons of this low correlation compared to other cases might be dry climate. For this reason there are too many zero rainfall values in a particular season and the computed SPI values for short timesteps may not be normally distributed (Mishra and Singh, 2010). Furthermore, due to the lack of soil moisture, harsh geology and reduced groundwater discharge may not replenish enough water for streamflow. It was also found from regression analysis that geology was one of the main factors affecting hydrological droughts (Vogel and Kroll, 1992; Van Loon and Laaha, 2015). Therefore, long term calculation of SSFI might be highly skewed and might not be well fitted by the gamma distribution. Li et al. (2018) investigated connections between meteorological and hydrological droughts in a semi-arid basin of Yellow River (China) and found that Pearson's correlation between Standardized Precipitation Evapotranspiration Index (SPEI) and SSFI (from one to 12-month timesteps) was found to be relatively low ($r_p < 0.6$) similar to our findings. Furthermore, Torabi Haghighi et al. (2020) found that Pearson's correlation coefficient between SPI and SRI (from 1 to 24-month timesteps) was less than 0.5 due to low precipitation and large evapotranspiration.

EDI, on the other hand, showed a decreasing correlation coefficient with hydrological drought index SSFI (Fig. 12b) as time increased, which is expected, since EDI has a high dissimilarity level from 6- to 12-month SPI (Dogan et al., 2012), and this similarity decreases after 9-month (Jain et al., 2015; Wable et al., 2019). However, EDI had a higher correlation ($0.58 < r_p < 0.84$) than SPI at 3-month timestep ($0.45 < r_p < 0.82$) with SSFI for all the five paired stations, especially in arid regions. This finding shows that EDI is capable to identify short term hydrological drought better than SPI. Similar to our findings, Dogan et al. (2012) also found that EDI is preferable to monitor meteorological drought in arid/semi-arid regions. Besides, we suggest that EDI and SPI might be used jointly to establish short-term hydrological drought for an early drought warning in semi-arid regions. Furthermore, combining and comparing different drought indices could help investigate correlation between them, characterize droughts, explore the accuracy and sensitivity of drought indices, and to delve into how well they cohere with each other in the context of a specific objective (Guttman, 1998; Szalai et al., 2000; Wu et al., 2001; Morid et al., 2006; Paulo and Pereira, 2006; Smakhtin and Hughes, 2007; Pandey et al., 2008; Dogan et al., 2012).

In addition to Pearson's correlation coefficient, we tested Spearman's rank correlation for the same paired stations to find the best accumulation period and we found consistent results to Pearson's correlation for both SPI/SSFI and EDI/SSFI (Fig. C3).

4.5. Propagation time from meteorological to hydrological drought

Table 8 presents the drought propagation time (DPT) with their duration, magnitude, intensity, and interarrival time at a paired station, 206025–56065, at 36-month timestep. It should be noted that only matched meteorological and hydrological drought events were identified by run theory as shown in Table 8. DPT is the lag time between the onset of hydrological drought and that of meteorological one. For instance, meteorological drought initiated in February 1993 and hydrological drought started in July 1993. Therefore, DPT which is lag time was found as 5 months for station 206025 (Table 8). It means that it takes about 5 months for the deficit of rainfall to be manifested in streamflow.

Table 8
Drought event pairs at 206025–56065 based on 36-month accumulation period by run theory.

Hydrological Drought						Meteorological drought						Lag Time (month)
Onset	End	D	M	I	IAT	Onset	End	D	M	I	IAT	
1981–12	1984–1	25	32.9	1.31		1980–2	1983–12	46	59.1	1.29		22
1993–7	1996–1	30	41.6	1.39	139	1993–2	1997–2	48	56	1.17	156	5
2001–9	2010–9	108	48.9	0.45	98	2001–9	2005–9	48	35.1	0.73	103	0
2014–11	2020–1	62	53.6	0.86	158	2014–1	2017–3	38	43.4	1.14	148	10
						2019–6	2020–1	7	6.6	0.94	65	

D: duration (month), M: magnitude, I: intensity, IAT: interarrival time (month)

Table 9 summarizes the list of hydrological and meteorological droughts along with their corresponding mean duration, magnitude, and interarrival times. The interarrival time of drought events is defined as the period of time from the initiation of a drought to the onset of a next drought event (see Fig. 3). The return period or recurrence interval of a hydrological drought can be considered as the average interarrival time of hydrological droughts with a certain magnitude or greater (Haan, 1977; Shiau and Shen, 2001). It should be noted that meteorological data set was paired with hydrological data set. Therefore, meteorological drought characteristics in Table 9 show pair-wise comparison with hydrological drought time period. Meteorological droughts were most frequent than hydrological droughts. Hydrological droughts had longer durations and magnitudes than meteorological droughts.

Despite the fact that we expect increasing DPT with time (accumulation period), but we could not find direct increasing DPT link with accumulation period after 12-month. We found increasing or decreasing DPT mainly after the 12-month accumulation period, since hydrological drought does not show a linear response to meteorological drought (Wu et al., 2017). However, mostly increasing DPT from meteorological to hydrological drought was found with time between 3 and 12 months (not shown). Wu et al. (2021) analyzed drought propagation time for 1-,3-, and 12-month timesteps in three sub-basins located in southern China with three hydrometric stations and they found that propagation time from meteorological to hydrological drought increased as time step increased. Although there is a strong linkage between meteorological drought and hydrological drought, it is challenging to generalize DPT due to the complexity of the nature of drought. Response sensitivity of hydrological drought from meteorological one can be different due to the impacts of other variables, such as soil moisture, evaporation, temperature, humidity, catchment characteristics, and human activities. For instance, DPT from meteorological drought to hydrological drought was estimated by some researchers (Edossa et al., 2010; Liu et al., 2012; Zhao et al., 2014; Wu et al., 2017) and their findings varied from 0.46 to 13. One of the main reasons for different estimated DPTs is climatic variability. As an illustration, short response time for DPT is expected in the humid region, whereas arid and semi-arid regions show longer response time of the hydrological process (Barker et al., 2016). All in all, by considering the aforementioned limitations DPT can be computed by 'theory of run' for regional water resources management and drought forecasting in the study area.

Table 9
Summary of hydrological and meteorological drought characteristics with average lag time of drought onset.

Drought Period		Hydrological drought				Meteorological drought			Lag Time (month)
		12-month							
	SF-ID	$\overline{D}$	$\overline{M}$	$\overline{IAT}$	R-ID	$\overline{D}$	$\overline{M}$	$\overline{IAT}$	
1979–2020	206025	33	30	91	56065	26	23	68	7.0
1972–2020	221002	31	27	76	69029	28	27	60	3.3
1982–2020	405241	33	37	99	88023	21	20	49	4.8
1972–2020	405245	25	27	77	83019	21	21	55	1.3
1965–2020	422002	36	32	89	48015	26	23	70	6.2
Drought		*24-month*							Lag
Period	SF-ID	$\overline{D}$	$\overline{M}$	$\overline{IAT}$	R-ID	$\overline{D}$	$\overline{M}$	$\overline{IAT}$	Time (month)
1980–2020	206025	31	33	113	56065	36	39	117	5.0
1980–2020	221002	50	42	112	69029	35	35	74	1.8
1982–2020	405241	90	90	190	88023	38	35	86	6.5
1977–2020	405245	59	54	146	83019	36	36	82	3.7
1980–2020	422002	53	52	100	48015	40	42	115	8.75
Drought		*36-month*							Lag
Period	SF-ID	$\overline{D}$	$\overline{M}$	$\overline{IAT}$	R-ID	$\overline{D}$	$\overline{M}$	$\overline{IAT}$	Time (month)
1981–2020	206025	56	44	132	56065	37	40	118	9.3
1981–2020	221002	86	77	220	69029	71	65	150	10.3
1982–2020	405241	96	94	196	88023	64	58	125	7.0
1998–2020	405245	111	101	183	83019	50	53	83	5.0
1966–2020	422002	57	53	146	48015	59	57	195	2.5

SF-ID: streamflow gauge ID, R-ID: rainfall gauge ID, $\overline{D}$: mean duration (month), $\overline{M}$: mean magnitude, $\overline{IAT}$: mean interarrival time (month)

5. Conclusions

The meteorological drought hazard can be identified by applying Thiessen polygons (Voronoi diagrams) as a conceptual index (DHI) which depicts the probability of drought and its severity in a non-dimensional spatial extent. Furthermore, the drought frequency index (DFI) can be estimated by associating the number of drought occurrences and length of time series. Spatial interpolation can then be used to identify zones that are 'vulnerable to drought.' Regional assessment of MDFI shows that Region-3 (Temperate), which has the highest annual average rainfall considering the whole study area, had the topmost level MDFI for any timestep SPI and EDI compared to Region-1 (arid) and Region-2 (semi-arid). Therefore, it is challenging to propose a relationship between rainfall distribution and potential drought zone. Hydrological DFI (HDFI) results show that "High" level HDFI was found at 3- and 6-month timesteps of SSFI. Consequently, higher HDFIs for each timestep of SSFI were detected in the south east coast and north of Murray-Darling Basin.

The major findings of this study are noted below.

1. Overall, the south and coastal zones of southeast Australia were detected as the most drought prone regions based on DHI, whereas higher level meteorological DFI (MDFI) were detected mainly in the east coast and southwest parts of the study area.
2. Decreasing abrupt change in annual total streamflow at 0.01 significance level was identified mainly in Victoria. The most dominant year of abrupt change was found to be 1996.

   Maximum hydrological drought characteristics, duration, magnitude, and intensity were found in the late-90 s and mostly 00 s based on 3-, 6-, 9-, 12-, and 36-month SSFIs. The percentage of total hydrological drought events and the severity mostly increased after 1990.
3. Hydrological droughts were found to be increasing at 0.01, 0.05 and 0.1 significance levels for all the selected timesteps of SSFI in southeast Australia.
4. Pearson's correlation and Spearman's rank correlation agreed that the highest correlation between SPI and SSFI was found at 12- and 24-month accumulation periods. Correlations of 36-month timestep were found to be inconsistent due to the limitation of data length and climate variability.
5. EDI was found to be inadequate for long term hydrological drought. On the other hand, EDI depicts a higher correlation (on both Pearson's and Spearman's rank) with 3-month SSFI compared to 3-month SPI. Furthermore, performance of EDI with SSFI was found to be better than SPI at 3-month timestep in semi-arid regions. Therefore, EDI and SPI can be used jointly in order to identify the onset of short-term hydrological drought, which could be convenient for an early warning system.
6. Due to the success of SPI and SSFI's capability in defining drought onset, drought propagation time (DPT) can be found from meteorological to hydrological drought by using the 'theory of runs'. However, defined DPT cannot be directly applied to other regions, since it is challenging to formulate or generalize DPT due to complexity of the nature of drought and catchment characteristics. Shorter timesteps of hydrological drought run into mostly shorter DPT and vice versa. However, response sensitivity of hydrological drought from meteorological drought can be different due to impacts of other variables, such as soil moisture, evaporation, temperature, humidity, catchment characteristics, and human activities. Overall, DPT can be computed by the 'theory of runs' for regional water resources management and drought forecasting in the southeast Australia.

This study can be extended to identify drought risk in southeast Australia by adding related vulnerability and exposure parameters. Besides, this comprehensive analysis can bridge the existing gaps in the current drought research and would be useful to identify the most vulnerable sub-areas to drought in order to help early drought warnings, water resources management, drought mitigation, and drought action plan. Furthermore, the findings of this study can be used to develop hydrological drought warning systems based on meteorological drought analysis.

Declaration of Competing Interest

The authors declare that they have no known competing financial interests or personal relationships that could have appeared to influence the work reported in this paper.

Data availability

The authors do not have permission to share data.

Appendix A. Supporting information

Supplementary data associated with this article can be found in the online version at doi:10.1016/j.ejrh.2022.101229.

References

Adisa, O.M., Masinde, M., Botai, J.O., 2021. Assessment of the dissimilarities of EDI and SPI measures for drought determination in South Africa. Water 13 (1), 82. https://doi.org/10.3390/w13010082.

AghaKouchak, A., Chiang, F., Huning, L.S., et al., 2020. Climate extremes and compound hazards in a warming world. Annu. Rev. Earth Planet. Sci. 48, 519–548.

Akhtari, R., Morid, S., Mahdian, M.H., Smakhtin, V., 2009. Assessment of areal interpolation methods for spatial analysis of SPI and EDI drought indices. Int. J. Climatol. 29 (1), 135–145. https://doi.org/10.1002/joc.1691.

Australian Bureau of Statistics, 2021. Water account, Australia, 2018–19. Cat. no. 4610.0 Canberra: ABS, 2021, viewed 10 June 2021, ⟨www.abs.gov.au/ausstats/abs@.nsf/mf/4610.0⟩.

Barker, L.J., Hannaford, J., Chiverton, A., Svensson, C., 2016. From meteorological to hydrological drought using standardised indicators. Hydrol. Earth Syst. Sci. 20 (6), 2483–2505. https://doi.org/10.5194/hess-20-2483-2016.

Blauhut, V., Gudmundsson, L., Stahl, K., 2015. Towards pan-European drought risk maps: quantifying the link between drought indices and reported drought impacts. Environ. Res. Lett. 10 (1), 014008.

Bond, N.R., Lake, P.S., Arthington, A.H., 2008. The impacts of drought on freshwater ecosystems: an Australian perspective. Hydrobiologia 600 (1), 3–16. https://doi.org/10.1007/s10750-008-9326-z.

Bryant, E.A., 1991. Natural Hazards. Cambridge University Press, Cambridge.

Bureau of Meteorology, 2020b. Water in Australia 2018–2019. Available from:⟨http://www.bom.gov.au/water/waterinaustralia/⟩.

Bureau of Meteorology, 2020a. Available from: ⟨http://www.bom.gov.au/climate/data/⟩.

Bureau of Meteorology, 2016. "Climate classification maps", Product Code: IDCJCM0000, viewed 15 January 2021, ⟨http://www.bom.gov.au/jsp/ncc/climate_averages/climate-classifications/⟩.

Byun, H.-R., Wilhite, D.A., 1999. Objective quantification of drought severity and duration. J. Clim. 12 (9), 2747–2756, 10.1175/1520-0442(1999)012<2747:oqodsa>2.0.co;2.

Caloiero, T., 2018. SPI trend analysis of New Zealand applying the ITA technique. Geosciences 8 (3), 101.

Cancelliere, A., Mauro, G.D., Bonaccorso, B., Rossi, G., 2007. Drought forecasting using the Standardized Precipitation Index. Water Resour. Manag. 21 (5), 801–819. https://doi.org/10.1007/s11269-006-9062-y.

Costa, A.C., Soares, A., 2009. Homogenization of climate data: review and new perspectives using geostatistics. Math. Geosci. 41 (3), 291–305.

CSIRO, 2010. Climate variability and change in south-eastern Australia: a synthesis of findings from Phase 1 of the South Eastern Australian Climate Initiative (SEACI).

CSIRO, BOM, 2020. State of the Climate.

Dai, A., 2021. Hydroclimatic trends during 1950–2018 over global land. Clim. Dyn. https://doi.org/10.1007/s00382-021-05684-1.

DELWP, 2020. Victoria State Government, Department of Environment, Land, Water and Planning, Available from: ⟨https://data.water.vic.gov.au/⟩.

Deo, R.C., Byun, H.-R., Adamowski, J.F., Begum, K., 2017. Application of effective drought index for quantification of meteorological drought events: a case study in Australia. Theor. Appl. Climatol. 128 (1–2), 359–379. https://doi.org/10.1007/s00704-015-1706-5.

Diffenbaugh, N.S., Singh, D., Mankin, J.S., et al., 2017. Quantifying the influence of global warming on unprecedented extreme climate events. Proc. Natl. Acad. Sci. USA 114 (19), 4881–4886. https://doi.org/10.1073/pnas.1618082114.

Dogan, S., Berktay, A., Singh, V.P., 2012. Comparison of multi-monthly rainfall-based drought severity indices, with application to semi-arid Konya closed basin, Turkey. J. Hydrol. 470–471, 255–268. https://doi.org/10.1016/j.jhydrol.2012.09.003.

Dracup, J.A., Lee, K.S., Paulson, E.G., 1980. On the statistical characteristics of drought events. Water Resour. Res. 16 (2), 289–296. https://doi.org/10.1029/wr016i002p00289.

Edossa, D.C., Babel, M.S., Das Gupta, A., 2010. Drought analysis in the Awash River Basin, Ethiopia. Water Resour. Manag. 24 (7), 1441–1460. https://doi.org/10.1007/s11269-009-9508-0.

Eslamian, S., Eslamian, F.A., 2017. Handbook of Drought and Water Scarcity: Environmental Impacts and Analysis of Drought and Water Scarcity. CRC Press.

Forootan, E., Khaki, M., Schumacher, M., et al., 2019. Understanding the global hydrological droughts of 2003–2016 and their relationships with teleconnections. Sci. Total Environ. 650, 2587–2604.

Gallant, A.J.E., Reeder, M.J., Risbey, J.S., Hennessy, K.J., 2013. The characteristics of seasonal-scale droughts in Australia, 1911-2009. Int. J. Climatol. 33 (7), 1658–1672. https://doi.org/10.1002/joc.3540.

Guttman, N.B., 1998. Comparing the palmer drought index and the standardized precipitation index. J. Am. Water Resour. Assoc. 34 (1), 113–121. https://doi.org/10.1111/j.1752-1688.1998.tb05964.x.

Haan, C.T., 1977. Statistical Methods in Hydrology. University, Press, Ames, IA.

Hajani, E., Rahman, A., 2018. Characterizing changes in rainfall: a case study for New South Wales, Australia. Int. J. Climatol. 38 (3), 1452–1462.

Hamed, K.H., Rao, A.R., 1998. A modified Mann-Kendall trend test for autocorrelated data. J. Hydrol. 204 (1–4), 182–196.

Hartkamp, A.D., De Beurs, K., Stein, A., White, J.W., 1999. Interpolation techniques for climate variables. Cimmyt.

Hawkins, D.M., 1977. Testing a sequence of observations for a shift in location. J. Am. Stat. Assoc. 72 (357), 180–186.

Hayes, M.J., Svoboda, M.D., Wilhite, D.A., Vanyarkho, O.V., 1999. Monitoring the 1996 drought using the standardized precipitation index. Bull. Am. Meteorol. Soc. 80 (3), 429–438, 10.1175/1520-0477(1999)080<0429:mtduts>2.0.co;2.

Helsel, D.R., Hirsch, R.M., 1992. Statistical Methods in Water Resources, 49. Elsevier.

Hughes, L., Steffen, W., Mullins, G. et al., 2020. Summer of crisis.

Jain, V.K., Pandey, R.P., Jain, M.K., Byun, H.-R., 2015. Comparison of drought indices for appraisal of drought characteristics in the Ken River Basin. Weather Clim. Extrem. 8, 1–11. https://doi.org/10.1016/j.wace.2015.05.002.

Jehanzaib, M., Shah, S.A., Kwon, H.H., Kim, T.W., 2020a. Investigating the influence of natural events and anthropogenic activities on hydrological drought in South Korea. Terr. Atmos. Ocean. Sci. 31 (1), 85–96. https://doi.org/10.3319/TAO.2019.08.13.01.

Jehanzaib, M., Shah, S.A., Yoo, J., Kim, T.W., 2020b. Investigating the impacts of climate change and human activities on hydrological drought using non-stationary approaches. J. Hydrol. 588. https://doi.org/10.1016/j.jhydrol.2020.125052.

Jenks, G.F., 1967. The data model concept in statistical mapping. Int. Yearb. Cartogr. 7, 186–190.

Kamruzzaman, M., Hwang, S., Cho, J., Jang, M.-W., Jeong, H., 2019. Evaluating the spatiotemporal characteristics of agricultural drought in Bangladesh using effective drought index. Water 11 (12), 2437. https://doi.org/10.3390/w11122437.

Kanellou, E., Domenikiotis, C., Blanta, A., Hondronikou, E., Dalezios, N., 2008. Index-based drought assessment in semi-arid areas of Greece based on conventional data. Eur. Water 23 (24), 87–98.

Kazemzadeh, M., Malekian, A., 2016. Spatial characteristics and temporal trends of meteorological and hydrological droughts in northwestern Iran. Nat. Hazards 80 (1), 191–210. https://doi.org/10.1007/s11069-015-1964-7.

Kchouk, S., Melsen, L.A., Walker, D.W., Van Oel, P.R., 2022. A geography of drought indices: mismatch between indicators of drought and its impacts on water and food securities. Nat. Hazards Earth Syst. Sci. 22 (2), 323–344. https://doi.org/10.5194/nhess-22-323-2022.

Kemter, M., Fischer, M., Luna, L.V., et al., 2021. Cascading hazards in the aftermath of Australia's 2019/2020 black summer wildfires. Earth's Future 9 (3). https://doi.org/10.1029/2020ef001884.

Kendall, M.G., 1975. Rank Correlation Methods. Oxford University Press, New York, NY.

Kiem, A.S., Johnson, F., Westra, S., et al., 2016. Natural hazards in Australia: droughts. Clim. Change 139 (1), 37–54. https://doi.org/10.1007/s10584-016-1798-7.

Kim, D.-W., Byun, H.-R., Choi, K.-S., 2009. Evaluation, modification, and application of the Effective Drought Index to 200-Year drought climatology of Seoul, Korea. J. Hydrol. 378 (1–2), 1–12.

Kim, H., Park, J., Yoo, J., Kim, T.-W., 2013. Assessment of drought hazard, vulnerability, and risk: a case study for administrative districts in South Korea. J. Hydro-Environ. Res. 9 (1), 28–35.
Kocsis, T., Kovács-Székely, I., Anda, A., 2017. Comparison of parametric and non-parametric time-series analysis methods on a long-term meteorological data set. Cent. Eur. Geol. 60 (3), 316–332. https://doi.org/10.1556/24.60.2017.011.
Kubiak-Wójcicka, K., Bąk, B., 2018. Monitoring of meteorological and hydrological droughts in the Vistula basin (Poland). Environ. Monit. Assess. 190 (11) https://doi.org/10.1007/s10661-018-7058-8.
Li, B., Zhu, C., Liang, Z., Wang, G., Zhang, Y., 2018. Connections between meteorological and hydrological droughts in a semi-arid basin of the middle Yellow River. Proc. Int. Assoc. Hydrol. Sci. 379, 403–407. https://doi.org/10.5194/piahs-379-403-2018.
Li, J., Wu, C., Xia, C.-A., et al., 2021. Assessing the responses of hydrological drought to meteorological drought in the Huai River Basin, China. Theor. Appl. Climatol. 144 (3–4), 1043–1057. https://doi.org/10.1007/s00704-021-03567-3.
Liu, L., Hong, Y., Bednarczyk, C.N., et al., 2012. Hydro-climatological drought analyses and projections using meteorological and hydrological drought indices: a case study in Blue River Basin, Oklahoma. Water Resour. Manag. 26 (10), 2761–2779. https://doi.org/10.1007/s11269-012-0044-y.
Lohpaisankrit, W., Techamahasaranont, J., 2021. Analysis of precipitation and streamflow data for drought assessment in an unregulated watershed. Environ. Nat. Resour. J. 19 (2), 18–27. https://doi.org/10.32526/ennrj/19/2020202.
Malik, A., Kumar, A., Kisi, O., et al., 2021. Analysis of dry and wet climate characteristics at Uttarakhand (India) using effective drought index. Nat. Hazards 105 (2), 1643–1662. https://doi.org/10.1007/s11069-020-04370-5.
Mann, H.B., 1945. Nonparametric tests against trend. Econometrica 13 (3), 245. https://doi.org/10.2307/1907187.
McKee, T.B., Doesken, N.J., Kleist, J., 1993. The relationship of drought frequency and duration to time scales. In: Proceedings of the 8th Conference on Applied Climatology, Boston, pp. 179–183.
Mishra, A.K., Desai, V.R., 2005. Spatial and temporal drought analysis in the Kansabati river basin, India. Int. J. River Basin Manag. 3 (1), 31–41. https://doi.org/10.1080/15715124.2005.9635243.
Mishra, A.K., Singh, V.P., 2009. Analysis of drought severity-area-frequency curves using a general circulation model and scenario uncertainty. J. Geophys. Res. 114 (D6) https://doi.org/10.1029/2008jd010986.
Mishra, A.K., Singh, V.P., 2010. A review of drought concepts. J. Hydrol. 391 (1–2), 202–216. https://doi.org/10.1016/j.jhydrol.2010.07.012.
Mishra, A.K., Singh, V.P., Desai, V.R., 2009. Drought characterization: a probabilistic approach. Stoch. Environ. Res. Risk Assess. 23 (1), 41–55. https://doi.org/10.1007/s00477-007-0194-2.
Modarres, R., 2007. Streamflow drought time series forecasting. Stoch. Environ. Res. Risk Assess. 21 (3), 223–233. https://doi.org/10.1007/s00477-006-0058-1.
Mondol, M.A.H., Zhu, X., Dunkerley, D., Henley, B.J., 2021. Observed meteorological drought trends in Bangladesh identified with the Effective Drought Index (EDI. Agric. Water Manag. 255, 107001 https://doi.org/10.1016/j.agwat.2021.107001.
Morid, S., Smakhtin, V., Moghaddasi, M., 2006. Comparison of seven meteorological indices for drought monitoring in Iran. Int. J. Climatol. 26 (7), 971–985. https://doi.org/10.1002/joc.1264.
Mpelasoka, F., Hennessy, K., Jones, R., Bates, B., 2008. Comparison of suitable drought indices for climate change impacts assessment over Australia towards resource management. Int. J. Climatol. J. R. Meteorol. Soc. 28 (10), 1283–1292.
Murphy, B.F., Timbal, B., 2008. A review of recent climate variability and climate change in southeastern Australia. Int. J. Climatol. 28 (7), 859–879. https://doi.org/10.1002/joc.1627.
Nazahiyah, R., Jayasuriya, N., Bhuiyan, M., 2014. Assessing droughts using meteorological drought indices in Victoria, Australia. J. Hydrol. Res.
Palmer, W.C., 1965. Meteorological drought. US Department of Commerce, Weather Bureau, Research Paper No. 45.
Pandey, R.P., Dash, B.B., Mishra, S.K., Singh, R., 2008. Study of indices for drought characterization in KBK districts in Orissa (India) 22 (12), 1895–1907. https://doi.org/10.1002/hyp.6774.
Paulo, A.A., Pereira, L.S., 2006. Drought concepts and characterization. Water Int. 31 (1), 37–49. https://doi.org/10.1080/02508060608691913.
Pearson, K., 1895. Notes on regression and inheritance in the case of two parents. Proc. R. Soc. Lond. 58, 240–242.
Pettitt, A.N., 1979. A non-parametric approach to the change-point problem 28(2) 126. DOI:10.2307/2346729.
Rahmat, S.N., Jayasuriya, N., Bhuiyan, M., 2012. Trend analysis of drought using standardised precipitation index (SPI) in Victoria, Australia, Hydrology and Water Resources Symposium 2012. Engineers Australia, pp. 441.
Rashid, M.M., Beecham, S., 2019. Characterization of meteorological droughts across South Australia. Meteorol. Appl. 26 (4), 556–568. https://doi.org/10.1002/met.1783.
Salarijazi, M., Akhond-Ali, A.-M., Adib, A., Daneshkhah, A., 2012. Trend and change-point detection for the annual stream-flow series of the Karun River at the Ahvaz hydrometric station. Afr. J. Agric. Res. 7 (32), 4540–4552.
Salimi, H., Asadi, E., Darbandi, S., 2021. Meteorological and hydrological drought monitoring using several drought indices. Appl. Water Sci. 11 (2) https://doi.org/10.1007/s13201-020-01345-6.
Schneider, S.H., 1996. Encyclopedia of Climate and Weather, 2. Oxford University Press, USA.
Sen, P.K., 1968. Estimates of the regression coefficient based on Kendall's Tau. J. Am. Stat. Assoc. 63 (324), 1379. https://doi.org/10.2307/2285891.
Shah, S.A., Jehanzaib, M., Yoo, J., Hong, S., Kim, T.-W., 2022. Investigation of the effects of climate variability, anthropogenic activities, and climate change on streamflow using multi-model ensembles. Water 14 (4), 512. https://doi.org/10.3390/w14040512.
Shiau, J.-T., Shen, H.W., 2001. Recurrence analysis of hydrologic droughts of differing severity. J. Water Resour. Plan. Manag. 127 (1), 30–40.
Shukla, S., Wood, A.W., 2008. Use of a standardized runoff index for characterizing hydrologic drought. Geophys. Res. Lett. 35 (2) https://doi.org/10.1029/2007gl032487.
Smakhtin, V., Hughes, D., 2007. Automated estimation and analyses of meteorological drought characteristics from monthly rainfall data 22 (6), 880–890. https://doi.org/10.1016/j.envsoft.2006.05.013.
Sönmez, F.K., Kömüscü, A.Ü., Erkan, A., Turgu, E., 2005. An analysis of spatial and temporal dimension of drought vulnerability in Turkey using the standardized precipitation index. Nat. Hazards 35 (2), 243–264. https://doi.org/10.1007/s11069-004-5704-7.
Spearman, C., 1904. The proof and measurement of association between two things. Am. J. Psychol. 15 (1), 72–101. https://doi.org/10.2307/1412159.
Spinoni, J., Naumann, G., Carrao, H., Barbosa, P., Vogt, J., 2014. World drought frequency, duration, and severity for 1951-2010. Int. J. Climatol. 34 (8), 2792–2804. https://doi.org/10.1002/joc.3875.
Szalai, S., Szinell, C., Zoboki, J., 2000. Drought monitoring in Hungary. Early Warn. Syst. Drought Prep. Drought Manag. 57, 182–199.
Talmi, A., Gilat, G., 1977. Method for smooth approximation of data, 23 (2), 93–123. https://doi.org/10.1016/0021-9991(77)90115-2.
Telesca, L., Lovallo, M., Lopez-Moreno, I., Vicente-Serrano, S., 2012. Investigation of scaling properties in monthly streamflow and Standardized Streamflow Index (SSI) time series in the Ebro basin (Spain). Phys. A Stat. Mech. Appl. 391 (4), 1662–1678. https://doi.org/10.1016/j.physa.2011.10.023.
Thiessen, A.H., 1911. Precipitation averages for large areas. Mon. Weather Rev. 39 (7), 1082–1089, 10.1175/1520-0493(1911)39<1082b:pafla>2.0.co;2.
Tian, F., Wu, J., Liu, L., et al., 2019. Exceptional drought across Southeastern Australia caused by extreme lack of precipitation and its impacts on NDVI and SIF in 2018. Remote Sens. 12 (1), 54. https://doi.org/10.3390/rs12010054.
Timbal, B., Fawcett, R., 2013. A historical perspective on Southeastern Australian rainfall since 1865 using the instrumental record. J. Clim. 26 (4), 1112–1129. https://doi.org/10.1175/jcli-d-12-00082.1.
Torabi Haghighi, A., Sadegh, M., Behrooz-Koohenjani, S., et al., 2020. The mirage water concept and an index-based approach to quantify causes of hydrological changes in semi-arid regions. Hydrol. Sci. J. 65 (2), 311–324. https://doi.org/10.1080/02626667.2019.1691728.
Trenberth, K.E., 2018. Climate change caused by human activities is happening and it already has major consequences. J. Energy Nat. Resour. Law 36 (4), 463–481. https://doi.org/10.1080/02646811.2018.1450895.
Ummenhofer, C.C., England, M.H., McIntosh, P.C., et al., 2009. What causes southeast Australia's worst droughts? Geophys. Res. Lett. 36 (4) https://doi.org/10.1029/2008gl036801.

Van Dijk, A.I.J.M., Beck, H.E., Crosbie, R.S., et al., 2013. The Millennium Drought in southeast Australia (2001-2009): natural and human causes and implications for water resources, ecosystems, economy, and society. Water Resour. Res. 49 (2), 1040–1057. https://doi.org/10.1002/wrcr.20123.
Van Lanen, H.A.J., Wanders, N., Tallaksen, L.M., Van Loon, A.F., 2013. Hydrological drought across the world: impact of climate and physical catchment structure. Hydrol. Earth Syst. Sci. 17 (5), 1715–1732. https://doi.org/10.5194/hess-17-1715-2013.
Van Loon, A.F., Laaha, G., 2015. Hydrological drought severity explained by climate and catchment characteristics. J. Hydrol. 526, 3–14. https://doi.org/10.1016/j.jhydrol.2014.10.059.
Van Oldenborgh, G.J., Krikken, F., Lewis, S., et al., 2021. Attribution of the Australian bushfire risk to anthropogenic climate change. Nat. Hazards Earth Syst. Sci. 21 (3), 941–960. https://doi.org/10.5194/nhess-21-941-2021.
Verdon-Kidd, D.C., Kiem, A.S., 2009. Nature and causes of protracted droughts in southeast Australia: comparison between the Federation, WWII, and Big Dry droughts. Geophys. Res. Lett. 36 (22) https://doi.org/10.1029/2009gl041067.
Vervoort, R.W., Dolk, M.M., Ogtrop, F.F., 2021. Climate change and other trends in streamflow observations in Australian forested catchments since 1970. Hydrol. Process. 35 (1) https://doi.org/10.1002/hyp.13999.
Vogel, R.M., Kroll, C.N., 1992. Regional geohydrologic-geomorphic relationships for the estimation of low-flow statistics. Water Resour. Res. 28 (9), 2451–2458. https://doi.org/10.1029/92wr01007.
Wable, P.S., Jha, M.K., Shekhar, A., 2019. Comparison of drought indices in a semi-arid river basin of India. Water Resour. Manag. 33 (1), 75–102. https://doi.org/10.1007/s11269-018-2089-z.
Wang, W., Shen, Y., Wang, F., Li, W., 2021. Two severe prolonged hydrological droughts analysis over mainland Australia using GRACE Satellite Data. Remote Sens. 13 (8), 1432. https://doi.org/10.3390/rs13081432.
Wasko, C., Shao, Y., Vogel, E., et al., 2021. Understanding trends in hydrologic extremes across Australia. J. Hydrol. 593, 125877 https://doi.org/10.1016/j.jhydrol.2020.125877.
WaterNSW, 2020. Available from: ⟨https://realtimedata.waternsw.com.au/⟩.
White, D.H., O'Meagher, B., 1995. Coping with exceptional droughts in Australia. Drought Netw. News 1994–2001, 91.
Wijngaard, J.B., Klein Tank, A.M.G., Können, G.P., 2003. Homogeneity of 20th century European daily temperature and precipitation series. Int. J. Climatol. 23 (6), 679–692. https://doi.org/10.1002/joc.906.
Wilhite, D.A., Glantz, M.H., 1985. Understanding: the drought phenomenon: the role of definitions. Water Int. 10 (3), 111–120.
World Meteorological Organization, W., 2012. Standardized Precipitation Index User Guide (M. Svoboda, M. Hayes and D. Wood). (WMO-No. 1090), Geneva.
Wu, H., Hayes, M.J., Weiss, A., Hu, Q., 2001. An evaluation of the Standardized Precipitation Index, the China-Z Index and the statistical Z-Score. Int. J. Climatol. 21 (6), 745–758. https://doi.org/10.1002/joc.658.
Wu, J., Chen, X., Yao, H., et al., 2017. Non-linear relationship of hydrological drought responding to meteorological drought and impact of a large reservoir. J. Hydrol. 551, 495–507. https://doi.org/10.1016/j.jhydrol.2017.06.029.
Wu, J., Chen, X., Yao, H., Zhang, D., 2021. Multi-timescale assessment of propagation thresholds from meteorological to hydrological drought. Sci. Total Environ. 765, 144232 https://doi.org/10.1016/j.scitotenv.2020.144232.
Yevjevich, V.M., 1967. Objective Approach to Definitions and Investigations of Continental Hydrologic Droughts. An, Colorado State University, Libraries.
Yildirim, G., Rahman, A., Singh, V.P., 2022. A bibliometric analysis of drought indices, risk, and forecast as components of drought early warning systems. Water 14 (2), 253. https://doi.org/10.3390/w14020253.
Yilmaz, A.G., Perera, B.J.C., 2015. Spatiotemporal trend analysis of extreme rainfall events in Victoria, Australia. Water Resour. Manag. 29 (12), 4465–4480. https://doi.org/10.1007/s11269-015-1070-3.
Zhang, X., Harvey, K.D., Hogg, W.D., Yuzyk, T.R., 2001. Trends in Canadian streamflow. Water Resour. Res. 37 (4), 987–998. https://doi.org/10.1029/2000wr900357.
Zhang, X.S., Amirthanathan, G.E., Bari, M.A., et al., 2016. How streamflow has changed across Australia since the 1950s: evidence from the network of hydrologic reference stations. Hydrol. Earth Syst. Sci. 20 (9), 3947–3965. https://doi.org/10.5194/hess-20-3947-2016.
Zhao, L., Lyu, A., Wu, J., et al., 2014. Impact of meteorological drought on streamflow drought in Jinghe River Basin of China. Chin. Geogr. Sci. 24 (6), 694–705. https://doi.org/10.1007/s11769-014-0726-x.
Zhao, P., Lü, H., Wang, W., Fu, G., 2019. From meteorological droughts to hydrological droughts: a case study of the Weihe River Basin, China. Arab. J. Geosci. 12 (11) https://doi.org/10.1007/s12517-019-4524-8.